Fatigue Damage Mechanisms of Advanced Hybrid Titanium Composite Laminates

A Thesis
Presented to
The Academic Faculty

by

Donald William Rhymer

In Partial Fulfillment
of the Requirements for the Degree
Master of Science in Mechanical Engineering

Georgia Institute of Technology
November 1999

REPORT DOCUMENTATION PAGE			Form Approved OMB No. 0704-0188

1. AGENCY USE ONLY *(Leave blank)*	2. REPORT DATE	3. REPORT TYPE AND DATES COVERED
	24.Jan.00	THESIS

4. TITLE AND SUBTITLE
FATIGUE DAMAGE MECHANISMS OF ADVANCED HYBRID TITANIUM COMPOSITE LAMINATES

5. FUNDING NUMBERS

6. AUTHOR(S)
CAPT RHYMER DONALD W

7. PERFORMING ORGANIZATION NAME(S) AND ADDRESS(ES)
GEORGIA INSTITUTE OF TECHNOLOGY

8. PERFORMING ORGANIZATION REPORT NUMBER

9. SPONSORING/MONITORING AGENCY NAME(S) AND ADDRESS(ES)
THE DEPARTMENT OF THE AIR FORCE
AFIT/CIA, BLDG 125
2950 P STREET
WPAFB OH 45433

10. SPONSORING/MONITORING AGENCY REPORT NUMBER
FY00-60

11. SUPPLEMENTARY NOTES

12a. DISTRIBUTION AVAILABILITY STATEMENT
Unlimited distribution
In Accordance With AFI 35-205/AFIT Sup 1

12b. DISTRIBUTION CODE

13. ABSTRACT *(Maximum 200 words)*

14. SUBJECT TERMS	15. NUMBER OF PAGES	16. PRICE CODE
	117	

17. SECURITY CLASSIFICATION OF REPORT	18. SECURITY CLASSIFICATION OF THIS PAGE	19. SECURITY CLASSIFICATION OF ABSTRACT	20. LIMITATION OF ABSTRACT

Fatigue Damage Mechanisms of Advanced Hybrid Titanium Composite Laminates

Approved:

W. S. Johnson

Prof. W. Steven Johnson, Chairman

Erian

Prof. Erian Armanios

David L. McDowell

Prof. David McDowell

Date Approved 24 November 1999

ACKNOWLEDGMENTS

I am eternally grateful to my Lord and Savior, Christ Jesus for salvation and working in me the patience and endurance to complete this work. "For from Him and through Him and to Him are all things." Rom 11:36 My wonderfully supportive fiancée, Dawn has helped me keep my focus on Christ first, others second, and self last which has made all the difference. I also thank my dear parents, sister and grandparents for their love and care throughout my lifetime of studies. The body of Christ at Heritage Church and at the A-1 house has been my family away from home, always ministering to me.

Special thanks and gratitude is extended to my advisor Dr. Steve Johnson for his direction, guidance, and support throughout this work. I would also like to thank the other members of my committee, Dr. Erian Armanios, Dr. David McDowell, particularly for sharing their expertise in composites and fatigue. I'm also grateful for Dr. T.L. St.Clair and Sharon Lowther at NASA-LaRC for the specimen construction and valuable inputs to the research. This project was supported by NASA under NAG-1-1890. Acknowledgement is extended to Cytec Fiberite in Havre de Grace, Maryland for the adhesive for tab bonding. Mr. Rick Brown has been invaluable with his machine testing patience and experience. Significant gratitude goes to the Air Force and DFEM, USAFA for this opportunity.

Finally, I thank my friends and colleagues Oh Chang Jin, Art Counts, Laurent Cretegny, Katie Lubke, Ted Cobb, Dave Clark, Kantis Simmons, Monica Hochstein, Tim Long, Russ Golden, and Major Larry Butkus who preceeded and continues to guide me.

TABLE OF CONTENTS

LIST OF TABLES

LIST OF FIGURES

SUMMARY

Hybrid Titanium Composite Laminates (HTCL) are a type of hybrid composite laminate with promise for high-speed aerospace applications, specifically designed for improved damage tolerance and strength at high-temperature (350°F, 177°C). However, in previous testing, HTCL demonstrated a propensity to excessive delamination at the titanium/PMC interface following titanium cracking. An advanced HTCL has been constructed with an emphasis on strengthening this interface, combining a PETI-5/IM7 PMC with Ti-15-3 foils prepared with an alkaline-perborate surface treatment. This thesis discusses how the room temperature tensile and fatigue capabilities of the "advanced" HTCL compare to the first generation HTCL which was not modified for interface optimization.

The tensile test results showed the advanced HTCL possesses a slight increase in stiffness over the initial laminate. This change was primarily a consequence of a minor variation in constituent volume fraction, as the advanced HTCL possessed a greater percentage of PMC layers due to being manufactured with titanium foil 0.0254 mm (1 mil) thinner than that used in the initial HTCL construction. The tests further validated the use of AGLPLY code to predict the stress-strain response.

Constant amplitude fatigue was conducted to monitor damage initiation, damage growth mechanisms, and to determine the fatigue life. The advanced HTCL under tension-tension (R = 0.1) appeared to show a modest fatigue life improvement in

comparison with previously tested initial HTCL results. However, this slight superiority can be attributed to the same difference in constituent geometry that affected the monotonic results and is, consequently, not beyond scatter and experimental variability. Comparing the number of cycles between the initial titanium ply damage and specimen failure showed a significant improvement (one order of magnitude for high cycle fatigue) in advanced HTCL due to interface strengthening. The damage progression following the initial ply damage (not performed on initial HTCL) demonstrated the effect of the strengthened PMC/titanium interface. Using acetate film replication of the specimen edges once titanium damage was evident, the advanced HTCL showed a propensity for some fibers in the adjacent PMC layers to fail at the point of titanium crack formation, suppressing delamination at the Ti/PMC interface. Following titanium ply cracking, these fibers would break and either a Mode I/Mode II (for outer ply damage) or Mode II (for inner ply damage) loading condition resulted in damage propagating longitudinally between the PMC fibers, rather then at the interface. The inspection of failure surfaces validated these findings, revealing PMC fibers to remain bonded to the majority of the titanium surfaces.

Tension compression fatigue (R = -0.2) was performed on both advanced and initial HTCL in this investigation and the strengthened interface was found superior in damage tolerance. Even though the fatigue lives were decreased for both HTCL constructions, the advanced HTCL endured a far greater number of cycles-to-failure following the initial titanium ply crack than initial HTCL at the same stress level due to resistance to delamination. Failure surfaces revealed a substantial amount of fibers

bonded to the titanium in advanced HTCL, while the initial laminate had few if any PMC fibers bonded. While overall fatigue life was not improved for either loading scenario, the damage mechanisms and subsequent failure modes were improved due to the strengthened interface of advanced HTCL.

CHAPTER I

INTRODUCTION

The envelope of advanced aerospace capabilities appears to be limited mainly by the material capabilities. As with any aerospace application, mechanical performance at minimal weight and cost continues to be a driving factor in the selection of materials. As a result, high-strength, low-weight aluminum has been the primary structural material used for aircraft production. But by the late 1960's, the first fiber-reinforced composites were making their way into military aircraft and their use in the industry has increased ever since.

While many engineering materials exhibit exceptional strength properties at minimal weight, damage and fracture must be understood in all cases. However, the solution is not always a matter of finding a completely new material. As composite research has shown, simply combining two or more already existing materials can produce a single material with the advantages of both while minimizing their disadvantages.

In recent years aerospace researchers have endeavored to meet the ongoing demands of both military and commercial aircraft to fly faster and longer then ever before. Such advancement is contingent upon structural materials capable of operating at long lives (> 10,000 hours) and higher temperatures while remaining fatigue resistant and

damage tolerant. Hybrid Titanium Composite Laminates (HTCL) are a type of hybrid laminate designed specifically for this purpose, possessing superior fatigue resistance and damage tolerance at temperatures up to 177°C (350°F). Comprised of varying layers of titanium alloy alternately bonded with layers of polymeric matrix composites (PMC), HTCL (also known as Titanium-Graphite Hybrid Laminates, or TiGr) has proven to possess exceptional strength and fatigue resistance at ambient or elevated temperatures, making it prime candidate for many advanced, high-speed aerospace applications.

However, initial results showed that HTCL consistently debonded at the titanium/polymer interface producing a highly unfavorable damage state [1]. When a fatigue crack forms in a titanium layer, the crack typically leads to complete failure of that ply and quickly tends to delaminate. To limit such damage, extensive research was conducted at Georgia Tech to determine the optimal combination of PMC resin and titanium surface treatment to adequately strengthen the interfacial bond between the HTCL layers [2]. The result of that research was the development a new, advanced HTCL, constructed with a PMC layer of PETI-5/IM7 bonded to alkaline-perborate treated Ti-15-3, designed specifically to reduce this interply delamination due to fatigue damage.

The objective of this thesis is to compare the mechanical response of this advanced HTCL to the first generation material. Specifically, the effect of a stronger bondline at the titanium/PMC interface in constant amplitude fatigue will be investigated, particularly in the event that titanium ply cracking induces the delamination. Therefore, the focus of this research is to closely monitor and analyze the damage progression of this

modified HTCL during fatigue testing to ultimately determine the specific damage evolution and mechanisms present. While tension-tension fatigue is conducted and compared to the previous HTCL testing, tension-compression fatigue is conducted on both laminates in this research as delamination effects are enhanced under compressive stresses.

The majority of the test matrix consisted of constant amplitude fatigue tests. Some tensile tests will be performed to determine the basic mechanical properties of the material. Though the development of HTCL is chiefly driven by an elevated temperature requirement, the testing will only be conducted on material at room temperature. This is done for two reasons: the previous HTCL testing at elevated temperature has been performed, and monitoring damage development in advanced HTCL is very different at elevated temperature. Elevated temperature testing previously demonstrated HTCL's fatigue durability at 177°C, the design requirements for HTCL [1]. Additionally, the equipment necessary for conducting elevated temperature tests in inhibits specimen surface accessibility to the during fatigue testing. With the central focus of this research being HTCL damage progression during fatigue loading, accessibility of the specimen edges of HTCL is essential. Moreover, the chief method for observing fatigue damage involves surface edge tape replication using acetone, necessitating a specimen that is not at an elevated temperature. For the purposes of this investigation, the HTCL modified for the current research will be referred to as "advanced HTCL," while the first generation material, to which the advanced will be compared, will be referred to as "initial HTCL".

CHAPTER II

LITERATURE SURVEY

Before presenting the current research, it is appropriate to review the history of previously performed related work. A literature survey was conducted to investigate the background of hybrid composites, their damage mechanisms, and the evolution of advanced HTCL.

2.1 Development of Hybrid Composite Laminate Systems

The development of HTCL is traced to research in strong, durable aerospace materials which offer superior mechanical performance yet are also damage tolerant. This history begins with a survey of the need beyond fiber-reinforced composites, leading to research in laminated metals, followed by their inevitable incorporation with fiber-reinforced composites into hybrid systems.

2.1.1 Weaknesses in Fiber-Reinforced Composites

In 1969, boron fiber-reinforced epoxy was utilized as the skin for U.S. Navy F-14 Tomcat's horizontal stabilizer [3]. That was the first significant production use of fiber-reinforced composites in the aircraft industry. By the mid-1970's, composites had

already been established in the engineering community as a premier design material of the future. Their superior strength-to-weight ratio and the capability of designing the material with direction-dependant properties with in-plane, mechanical superiority made such composites a prime candidate to replace aluminum and other lightweight metals, particularly in modern aerospace applications.

However, this replacement has been hampered by several weaknesses fiber-reinforced composites possess that are strengths of most aerospace metals. Though perhaps minor and not applicable for many structural applications, these weaknesses prove significant in many aircraft structures, inhibiting complete metal component replacement by composites. Among the more minor shortcomings, composites prove not near as durable as metals, particularly in aggressive environments. Most notably, the effects of heat and moisture can significantly alter and/or degrade a composite's mechanical properties [4]. Some damage in composites is difficult to find and always difficult to repair. For instance, given an impact, delamination can persist within the material requiring sophisticated equipment to detect [5]. Moreover, once damage is detected, composites become much more complicated to repair than metals, even if damage occurs on the surface. Fiber-reinforced composites are also extremely sensitive to lightening strikes, as they conduct electricity very poorly.

The major disadvantage of composites, which is at the root of many applications, is their lack of ductility and formability. Fiber-matrix composites are inherently brittle, possessing little-to-no toughness or yielding, particularly in comparison to metals. Carbon fibers are known to exhibit a much lower strain to failure than high strength

metals. This disadvantage manifests itself in several ways. Their brittle nature make composites extremely sensitive to machining and forming, two distinct advantages of metals, particularly in aircraft repair [4]. Secondly, composites can be less forgiving following impact damage. While metals absorb impact with often little significant damage, composites normally damage with resin failures and delamination between plies that are vital to the material structural integrity [5]. Even incorporating an epoxy matrix with relatively more ductility than the extremely brittle fiber, such composites still lack the valuable toughness found in metals since the fibers have a low strain to failure.

But lastly and perhaps most importantly, this lack of ductility has a significant effect on the damage tolerance and notch root plasticity of composites [4]. This is a major issue in modern aircraft design as all structures inevitably incur some damage and fracture and the inability to absorb such damage prevents widespread usage. Damage tolerance is the ability to resist complete material failure after sustained usage in the presence of flaws, cracks, or other damage. Cracks can exist in a component and it can remain safe and useable as long as the crack does not grow to a critical size. The study of fracture mechanics and its importance led to the incorporation of damage tolerance into aerospace design philosophy by the U.S. Air Force in 1974, followed by the Federal Aviation Administration (FAA) and Federal Airworthiness Regulations (FAR) in 1978 [6]. Consequently, soon after the Air Force selected it as its mainline advanced fighter in 1975, the F-16 became the first airplane designed according to damage tolerance specifications and is still flying today in the U.S. and 18 other nations around the world [7]. Some materials are not only damage tolerant, but are "fail safe", or able to withstand

detectable damage before catastrophic failure. And with the significant cost of inspections and repair, the more fail-safe a material is proven to be, the more economic it is to use.

All of these properties are significant to any aerospace application. Though the use of fiber-reinforced composites is still extremely valuable and in many applications optimal, some of these disadvantages preclude their extensive structural use in many aerospace applications.

2.1.2 Laminated Metals

The ductility, inspectability, machinability, impact absorption, electrical resistance, and environmental durability are all properties most structural metals, like aluminum, have long been known to possess. However, damage tolerance is an attribute that has only been in focus for the past thirty years.

One of the major developments in resisting such damage came in the form of laminating materials. In 1967, J. Kaufman [8] proved that a laminate of adhesively bonded aluminum plies has nearly twice the fracture toughness of a single aluminum plate of the same overall thickness. Using center cracked panels of 7075-T6, -T651, he showed that eight 0.063 in thick plies of aluminum adhesively bonded together (for a total thickness of 0.5 in) has approximately twice the fracture toughness of a monolithic panel 0.5 in thick. The reason for such an increase in toughness was due to the degree of plane-strain fracture. Because the thinner foils experience less plane strain than thicker material, a greater percentage of the material at failure is in shear. Therefore, when bonded together using adhesives, multiple layers of these sheets retard crack growth

because of these shear fracture surfaces. Kaufman went on to show that when a metallurgical bond is created, this fracture toughness advantage significantly diminishes.

In 1978 W. S. Johnson et al. [9] demonstrated the superior damage tolerance of a center-cracked ply bonded to multiple, uncracked plies. They showed that slower crack growth results because the load in the cracked ply is transferred to the uncracked plies through the adhesive in fatigue loading. When this is accomplished the stress intensity at the crack tip is reduced by the adhesive bond, which restrains the crack from opening. Additionally, they tested multiple geometries, varying the numbers of bonded plies and showed that increasing the number of plies reduces the crack growth rate.

Johnson [10], in 1983, proved these increased damage tolerant properties were not just limited to fatigued aluminum laminates, but characterized adhesively bonded titanium as well. Titanium is well known for its high strength-to-weight properties but is also much stronger than aluminum at higher temperatures. As a result, it is optimal material for high-speed aerospace applications. However, it is not, in monolithic form, very damage tolerant and is extremely notch sensitive. But by creating a laminate of 6-ply Ti-6Al-4V, the through-the-thickness fracture toughness was improved by almost 40%, where the laminate could sustain a crack nearly twice the length of one in a monolith. The crack growth rates were reduced by 20% in the laminate, and the damage tolerance life of a surface-cracked laminate ranged from 6 to 15 times that of the monolithic titanium.

2.1.3 Development of Hybrid Composite Laminates

Though there are not many applications for laminating metal sheets to each other, the point was clearly made that for fatigue dominant structures, adhesively laminating materials provides superior resistance to crack growth by the plane stress condition in thin metal sheets. Cracks must overcome the ductile sheer lip at several surfaces before catastrophically failing the entire laminate. Yet, metals still lacked the significant strength properties fiber composites afforded. Therefore, researchers at the Delft University of Technology in the Netherlands in the 1970's began to design a more advanced composite material which would retain the benefits of fiber-reinforced composites and laminated metal while greatly improving the fatigue crack growth rate and damage tolerance of both [11]. The result was the first hybrid composite laminate.

In 1978, Professor L.B. Vogelsang and colleagues [11] at Delft first developed ARALL by laminating alternating thin aluminum alloy sheets with aramid-reinforced adhesive prepreg. By 1983, the first production quality ARALL was being manufactured with ALCOA and significant testing has steadily increased ever since [4]. After the initial success of ARALL, a second-generation hybrid composite was developed called GLARE in 1991. AKZO (a major manufacturer of fibers and chemicals) in conjunction with ALCOA and Delft utilized the same theory incorporating this similar material which uses R and S2 glass instead of aramid as the fiber material to generate a hybrid composite laminate with a higher strain to failure [12].

These hybrid composites materials are laminated together under a high temperature cure cycle just as most fiber-reinforced composites. It possesses the high

specific properties of composites while retaining the ductility, machinability, weldability, inspectability, reparability, impact resistance, notch sensitivity, and environmental durability of metals [4]. One of the major reasons these metal advantages are incorporated into this material is by the placement of metal layers on the exterior of the laminate.

Other aluminum based hybrid laminates have been developed with more limited use. ALOR utilizes aluminum/organoplastic composites reinforced with aramid fibers to create a high fracture-toughness material [13]. Further research led to the development of CARALL and ALLIC which combined carbon fiber-reinforced plastics to aluminum and aluminum/lithium respectively [14].

The early successes of ARALL and GLARE have heightened the superior capabilities of hybrid composites as candidates for such use in fatigue driven materials. However, for future, high-speed aircraft, even more advanced materials are required. Researchers at NASA have determined the operating temperatures for the High-Speed Research program (HSR) to reach 177°C (350°F). This temperature range exceeds a level at which aluminum is able to retain its strength. With both of these early laminates possessing aluminum exteriors, ARALL and GLARE prove inadequate for such applications. To meet the need for a strong, lightweight, damage tolerant, and high-temperature material, a hybrid composite laminate composed of titanium, graphite fibers and high-temperature epoxy was manufactured as hybrid titanium composite laminate (Figure 2.1) [15]. HTCL was originally designed with the specific application of a potential skin material for the High Speed Civil Transport program. Another name for

HTCL is TiGr, which is an acronym bearing the names of the major constituents: Titanium and Graphite.

2.2 Previous HTCL Research

In the early 1990's, Miller et al. [15] conducted a preliminary analysis of the first HTCL laminates. Using 6 layers of Ti-6Al-4V titanium and 5 layers of graphite-reinforced PMC, they demonstrated that HTCL exceeded monolithic titanium in strength, stiffness, and damage tolerance. At both room temperature and at 177°C, HTCL showed significant improvement in fatigue life and crack growth resistance over the titanium alone. Crack growth through the laminate thickness was observed to be faster initially in the outer titanium plies, but the crack growth rate would slow down as the crack tip encountered the interfaces between the plies, producing and overall longer fatigue life. Additionally, Miller et al [15] determined the monotonic tensile response of HTCL could be accurately predicted using an elastic-plastic laminate prediction code AGLPLY.

Extensive HTCL testing was conducted by Li and Johnson [1] to validate the superior tensile strength and fatigue life determined by Miller [15]. Using two beta-stable titanium alloys (Ti-15-3 and Timetal-21S) combined with a PMC layer comprised of LARC-IAX (a high temperature polyimide) and IM7 graphite fibers, Li et al. showed HTCL of different compositions demonstrated an improvement in fatigue life over titanium alone. Moreover, at elevated temperature (177°C), HTCL performed even better

in fatigue than at room temperature due to the relief of residual stresses induced in the titanium layers during processing.

However, Li et al. [1] discovered that a recurring, undesirable failure mode was found to be delamination of the adhesively-bonded plies from the titanium foils. Interlaminar delamination has been researched determined an extremely detrimental damage mode in laminated composites, particularly in compression, due to its tendency to induce buckling along with the difficulty in its detection [16, 17]. For hybrid composite laminates, Miller et al. [15] showed that while a high interface bond strength between the titanium and the polymer matrix composite (PMC) is ideal for optimal load transfer, a lower bond strength can lead to an improved fatigue life. The debonding mode of failure was previously observed during the mechanical testing of ARALL, and was a focus of study for Verbruggen and Marrisen [11, 18]. However, as was proved by researchers at Delft, there is a balance in how low this bond strength can be before delamination becomes undesirable [18]. In the initial tests of HTCL, it became apparent that this lower limit had been reached.

2.3 Fatigue Damage Mechanisms in Hybrid Composite Laminates

To better understand how to prevent delamination of hybrid composite laminates, an investigation into the mechanics of fatigue damage in such a unique material is necessary. As previously noted, researchers at Delft and Alcoa pioneered the first hybrid composite laminates. In doing so, significant investigation into the mechanics and

progression of damage inherent to these materials was accomplished. After the initial development of ARALL at Delft, significant research was conducted by Marrisen [18] to characterize the damage tolerance inherent to the ARALL design. As with most hybrid composite laminates, damage development in ARALL typically initiates with the development of a fatigue crack in the metal lamina after a certain number of cycles while the composite layer, particularly the fibers, remain intact [11]. It is from this point, the damage progression is analyzed.

2.3.1 Crack Growth Model

Marrissen [18] first identified that the crack growth rate in ARALL could be modeled similarly to that of monolithic aluminum. The da/dN was still correlated to the stress intensity factor, only one that is adjusted for the effects of fiber bridging, delamination, adhesive shear deformation, specimen geometry, and residual stresses. In this investigation, Marissen determined fiber bridging was a major mechanism in increasing fatigue crack growth resistance and, subsequently that there was a relation between the amount of fiber bridging and the amount of delamination and adhesive shear deformation.

2.3.2 Fiber Bridging

Marrisen [18] showed that when a fatigue crack develops in the metal layer, the fiber-reinforced composite layers which will remain intact in the wake of the crack due to load transfer of the adhesive between the two. As a result, the fibers reduce the stress

intensity at the metallic crack tip by retarding further crack tip opening and fatigue crack propagation is slowed [19, 20]. This phenomenon is known as fiber bridging as the fibers "bridge" the wake of the crack and can thus absorb some of the energy given up by the metal.

Fiber bridging is integral to the fatigue damage success of hybrid composite laminates and is the chief mechanisms responsible for the high damage tolerance of the material. However, it is not desired, as Marissen [18] continued, to have what is known as "perfect fiber bridging". To illustrate his point, a hybrid composite laminate was considered at Delft as shown in Figure 2.2, whereby a starter notch or through crack is present in a center-notched panel with a fatigue crack over a certain distance (with fibers remaining intact) on either end of the notch. Given perfect bonding between the layers of each material and an infinite shear modulus in the adhesive PMC matrix, the crack tip stress intensity factor would effectively be zero. Though an apparently favorable condition (with the crack propagation in the metal), the stresses not carried by the metal are transferred to the fibers at the notch root leading to rapid fiber failure from the notch root to the crack tip. The crack would thus "unzip" and catastrophic failure would ensue. So for desirable fiber bridging, other mechanisms are needed to absorb more of the fatigue stresses [18]. The fortunate reality is that neither a perfectly rigid bond nor an infinitely stiff shear modulus exists, such that delamination and adhesive shear deformation result. These additional mechanisms which are necessary for adequate damage tolerance.

2.3.3 Delamination

In a hybrid composite laminate, the stresses carried by the fibers in the wake of the crack are transferred from the aluminum to the fibers via the adhesive bond between the two layers just above and below the crack in areas called crack flanks. When this stress now across the adhesive reaches a certain level, mixed mode (Mode I/Mode II) damage results in delamination and no additional load due to the cracked metal can be transferred to the fibers (See Fig. 2.3). This results in a lower crack bridging stresses and, thus allows some crack tip opening [18]. The larger the delamination area, the more crack opening and subsequent crack growth. It is important to note that as delamination occurs, some of the concentrated stresses in the fibers due to fiber bridging are relieved. But obviously, a limit is needed to the amount of delamination that is acceptable. Rapid, massive delamination would not only eliminate the benefits of fiber bridging, but are highly undesirable in any aerospace application and are likely catastrophic under compressive stresses. Therefore, controlled delaminations result in desirable, stable crack growth.

2.3.4 Adhesive Shear Deformation

Not only does delamination occur, but Marissen [18] also discovered the adhesive layer which bonds the matrix of the composite to the metal sheet deforms in shear due at the delamination boundary. Based on the shear modulus of the adhesive resin itself, this deformation is desirable within certain limits. As mentioned, an infinite modulus would

likely add considerable stress to the bridging fibers. However massive deformation, like delamination, nullifies any fiber-bridging effectiveness.

Ritchie, et al. [19] using compact ARALL specimens in fatigue, validated Marrisen's findings. He verified the claims of Delft and Marrisen that fiber bridging was successful when promoted by controlled delaminations and that a significant "bridging zone" of 3-5 mm resulted. J. Macharet [21] of ALCOA Laboratories conducted an extensive research on the delamination shape in ARALL and showed that the larger the delamination area in the longitudinal direction, the less effective the fibers are in bridging and slowing crack growth. Davidson and Austin [20], using single edge notched specimens of ARALL, also showed a marked superiority of ARALL over monolithic aluminum due to fiber bridging at high ΔK levels. Figure 2.4 shows the effect of both delamination and shear deformation at the crack flanks in adhesive in the presence of fiber bridging. As mentioned, there is a balanced medium in the amount of such damage that is desirable for effective fiber bridging efficiency in a hybrid composite laminate [18].

2.4 Investigation for HTCL Improvements

With the predominant failure mode of the initial HTCL being delamination between the PMC plies and the titanium foils, efforts began to determine ways to increase the strength of the titanium/PMC interface. Cobb and Johnson [2] conducted research on the integrity of the bonding between the two to be incorporated in a second-generation,

advanced HTCL. Cracked lap shear specimens were constructed with one of two different polymeric resins (LaRC-IAX and FMx5) bonded to Ti-15-3 with one of three commercially available titanium surface treatments (Pasa-Jell 107, Sol-Gel, and Turco 5578). The LaRC-IAX/Pasa-Jell was the combination used in the initial HTCL research by Li [1]. The FMx5 polyimide adhesive bonded with Boeing's Sol-Gel surface treatment possessed superior fracture toughness and fatigue crack growth, far greater than that of LaRC-IAX/Pasa-Jell, in a variety of exposure environments. Cobb's method of interface testing was based on crack growth using the strain energy release rate, which Burianek and Spearing [22] directly related to delamination growth in HTCL, as with other PMC's. Based on Cobb and Johnson's work [2], advanced HTCL was manufactured leading to the current research. The specific composition and fabrication methodology of the laminate is discussed in the following chapter, including the impact of Cobb's findings.

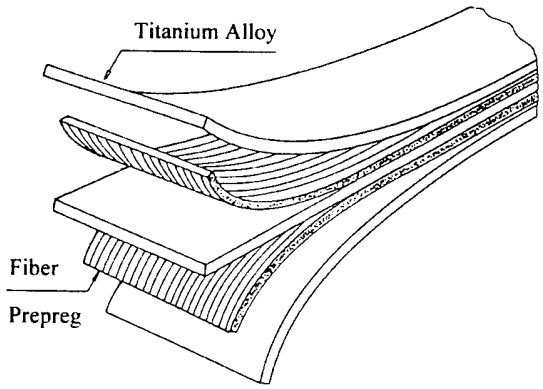

Figure 2.1 Hybrid Titanium Composite Laminate (HTCL)

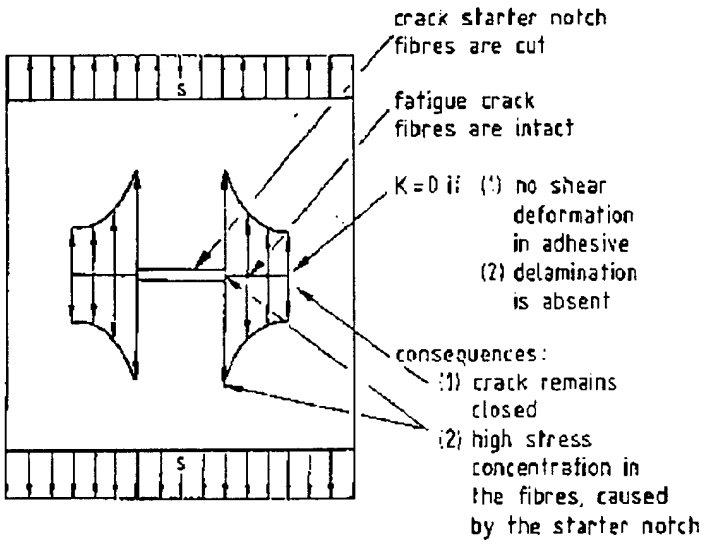

Figure 2.2 Marissen's schematic showing the stress concentrated on fibers near the metal crack resulting from perfect fiber-bridging in hybrid composite laminates (ref. [18])

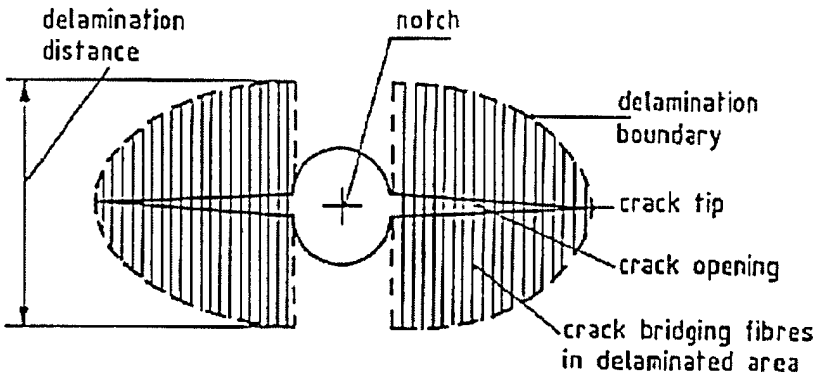

Figure 2.3 Schematic depicting delamination region for typical hybrid composite laminate (ref. [18])

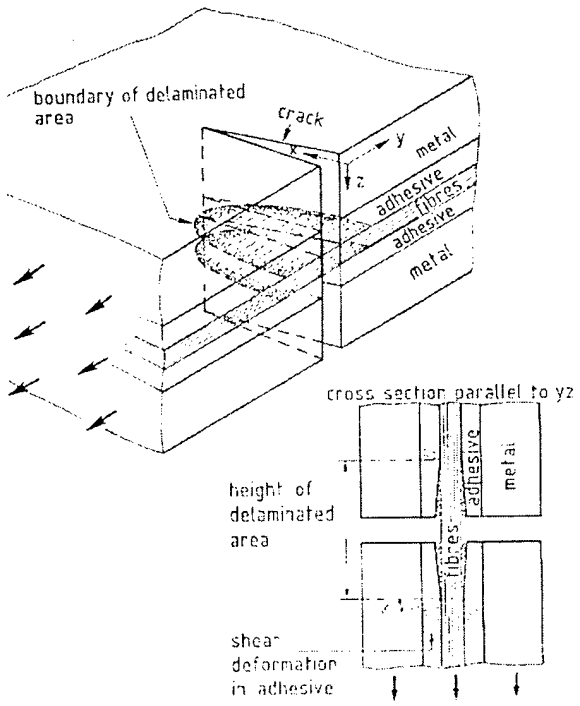

Figure 2.4 Schematic by Marissen showing damage mechanisms in hybrid composite laminates. Delamination with adhesive shear deformation inset (ref. [18])

CHAPTER III

PROCESSING

The processing for the HTCL fabrication took place at NASA-Langley Research Center (NASA-LaRC) in Hampton, Va. The PMC prepreg, titanium surface treatment solution, and autoclave were provided by NASA as well with the oversight of Sharon Lowther. The titanium coil was provided by TiComp which was accomplished the heat treatment and aging before shipment.

3.1 Constituent Materials

All HTCL used in this study is comprised of 4 plies of titanium foil and 3 plies of PMC. This combination was chosen simply for comparison with the previous HTCL research, which was of this construction.

3.1.1 Titanium

The titanium alloy used in this research was Ti-15V-3Cr-3Sn-3Al (Ti-15-3). Ti-15-3 is a high-strength, high temperature, cold-formable alloy. It was developed as a potential aerospace material in the 1970's to be more cost effective to produce than existing alloys such as Ti-6Al-4V and Ti-13V-11Cr-3Al. [23] This was achieved in cold

formability which allows it to be deformed, strip produced, and rolled into coils without hot forming, greatly reducing its production cost [23, 24]. Such formability is accomplished by its beta precipitate stability, where an all beta phase grain structure is produced and then is subsequently solution treated and aged to form finitely distributed alpha precipitates within the beta grains. The heat treatment of the Ti-15-3 used in this research is given in Table 3.1, including temperature and duration parameters for the solution treatment and aging process.

The titanium foils were cold rolled to a final thickness of 0.254 mm (10 mil) for HTCL fabrication. It is important to note that while the heat treatment and the titanium alloy incorporated in this advanced HTCL is identical to that of the initial HTCL, the initial laminate contained Ti-15-3 foil that was 0.279 mm (11 mil) thick. These differences can be noted via comparison of the micrographs of each in Figures 3.1 and 3.2, respectively.

3.1.2 PMC prepreg

The polymer resin used in the PMC layer was a thermomechanically stable polyimide adhesive called PETI-5 [25]. Developed at NASA-LaRC, PETI-5 is a phenylethynyl terminated imide oligomer which exhibits excellent mechanical properties and good processibility with an average molecular weight of 5000 g/mol. It is noteworthy that FMx5 (the polyimide Cobb et al [2] determined superior when coupled with the appropriate titanium surface treatment) is comprised of 70% PETI-5 and thus many of the same durability qualities are realized.

Within the PETI-5 resin, carbon IM7 fibers were embedded with approximately 0.6 volume fraction prior to cure. Following HTCL fabrication, the volume fraction became more closely approximated at 0.57.

3.2 HTCL Fabrication

The manufacturing of HTCL used in this analysis was conducted by Sharon Lowther and NASA-LaRC with the assistance of the author. The titanium was cut from a coil 17 cm (6.7 in) wide. Sections of the coil were cut at lengths of 8.9 cm (3.5 in) from the coil. This size (17 cm x 8.9 cm) governed the laminate size, thus the sheets of PETI-5/IM7 prepreg were cut to the same size as the Ti-15-3 plates. The titanium preparation involved surface treatment, conducted prior to bonding, and is discussed below. Since this surface treatment has proven an integral aspect of the current research in the effort to reduce delamination, a detailed analysis is provided.

The only pre-fabrication preparation necessary for the PMC prepreg was to be placed in a forced-air oven for one hour at 230°C (446°F) to evaporate some of the volatiles.

3.2.1 Titanium surface treatment

Before actual lamination of the prepreg with the titanium, the Ti-15-3 required surface treatment in order to effectively bond with the PMC resin. The treatment chosen for the current research was an alkaline-perborate surface treatment, which was

developed as a result of the prior work conducted by Cobb and Johnson [2]. Recall that he determined that Boeing's Sol-Gel process was optimal for the surface treatment of titanium, particularly when coupled with FMx5. Of specific note in Cobb's investigation was the determination that the Pasa-Jell 107 surface treatment in combination with the LaRC-IAX polyimide (the combination used in the initial HTCL construction) proved to possess a very low fracture toughness and resistance to crack growth along the bondline in ambient and aggressive exposure environments. It was determined that Pasa-Jell has the dilemma that the titanium dioxide surface that is formed has poor stability/durability under wet conditions. This oxide tends to form hydrates which results in a volume change in the oxide layer, which in turn leads to a build-up of stresses in the adhesive-to-oxide bond [26]. Of course, without an oxide present, the situation becomes even worse as the titanium surface eventually is exposed to water and oxygen and an oxide layer will form which will result in catastrophic bond failure.

Developed at Boeing to produce an environmentally stable (stable to hot-wet conditions) epoxy adhesive bonding to titanium, Sol-Gel produces a titanium surface more resistant to water intrusion because it has a 'ceramic' character when bonded. Such character is defined by being a "more stable mixed metal oxide", [26] containing silicone dioxide in addition to the titanium dioxide. However, though proven in Cobb's work [2] to be much improved over Pasa-Jell, the problem was that Boeing used a chemical coupling agent affording compatability for the epoxy in their Sol-Gel process. This coupling agent proved not chemically compatible with FMx5 nor PETI-5 and resulted in poor thermo-oxidative stability even though the initial hot-wet strengths were good.

With this process not yet optimized at the time of the present research, an alternative titanium surface treatment was utilized.

Many years ago, the Royal Aircraft Establishment (RAE) in England proved that an alkaline/peroxide generated oxide layer had superior environmental stability over the acidic Pasa-Jell treatment [26]. The problem with the RAE treatment is that 30% hydrogen peroxide must be used in combination with a strong alkaline base like sodium hydroxide. Because 30% hydrogen peroxide is hazardous for use in most commercial applications, Boeing refused to adopt this treatment. Dr. Terry St.Clair [26] at NASA-LaRC developed an alkaline/perborate treatment whereby a sodium perborate is employed as a safe carrier of hydrogen peroxide. This produced an alternative oxidizing method to 'chemically' generate hydrogen peroxide. Though not producing the ceramic-like surface as Sol-Gel, this treatment possesses superior environmental stability over the acidic Pasa-Jell treatment as used in the initial HTCL construction. Therefore, in lieu of the current uncertainties with Sol-Gel, the alkaline-perborate solution was used to prepare the titanium surface, which proved cost-effective, environmentally friendly, and chemically compatible with PETI-5.

The steps for the alkaline-perborate treatment of the titanium are as numbered below:

1. Wash with acetone
2. Brush thoroughly with an abrasive sponge
3. Wash with methyl alcohol
4. Wash in Dynasol solution

5. Etch in sulfuric acid for 15 minutes
6. Clean in ultrasonic bath for 5 minutes
7. Soak in perchloric acid for 10 minutes
8. Repeat step 6
9. Dry in forced-air oven at 100°C (212°F) for 10 minutes
10. Prime with 15% solution of a PETI-5
11. Dry in forced-air oven at 220°C (428°F) for one hour.

3.2.2 HTCL Consolidation

Following the cutting and treatment of the constituents, the HTCL assembly was cured via an autoclave, similar to most PMC's. In the extensive research conducted by Li [27] on the initial HTCL, he determined that the autoclave method of fabrication produced a much better quality laminate than by bonding the constituents using hot pressing. HTCL cured in an autoclave possessed a much more consistent thickness along the dimensions of the laminate, successfully maintained unidirectional fiber orientation, and produced far fewer voids and resin rich areas. As expected, the laminates fabricated in the autoclave, therefore, demonstrated much more consistent mechanical results.

For the autoclave curing, the laminate assembly of 4 Ti/3 PMC was arranged on a large flat die mold plate with a plate the size of the laminate on top to help maintain even pressure distribution and alignment. TX1040 release cloth was used to prevent the laminate from adhering to the mold plate. The HTCL was then placed in an autoclave bag whereby the laminate assembly was sandwiched and sealed between Kapton film. The

entire consolidation is shown on the die mold plate in Figure 3.3. The autoclave at NASA-LaRC for curing is shown in Figure 3.4. The following are the steps of the cure cycle:

1. Vacuum the HTCL assembly under 30 psi
2. Elevated temperature to 275°C (527°F) at ~ 0.87°C (2.1 °F) /min
3. Hold at 275°C (527°F)for 1 hour
4. Increase autoclave pressure to 1 MPa (150 psi) while increasing the temperature to 371°C (700°F) at a rate of ~1.31°C(2.9°F)/min
5. Hold at 371°C (700°F)for 1 hour
6. Decrease autoclave pressure to 172 Pa (25 psi) and decrease to room temperature at a rate of ~2.14°C (4.4°F)/min
7. Release pressure

One laminate consisting of one ply of Ti-15-3 and one ply of PMC prepreg was cured in the same manner for residual stress calculations. The background for the test and resultant calculations are discussed in Section 6.1.

Table 3.1 Heat Treatment for Ti-15-3

SOLUTION TREAT	COOLING	AGING TEMPERATURE	AGING PERIOD
788°C (1450°F) – 816°C (1500°F)	air cooled	510°C (950°F)	8 hours

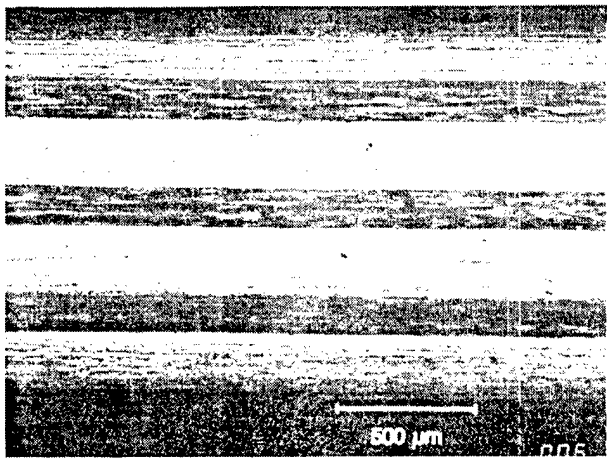

Figure 3.1 Magnification (50 X) of advanced HTCL cross section manufactured with 0.254 mm (10 mil) thick Ti-15-3

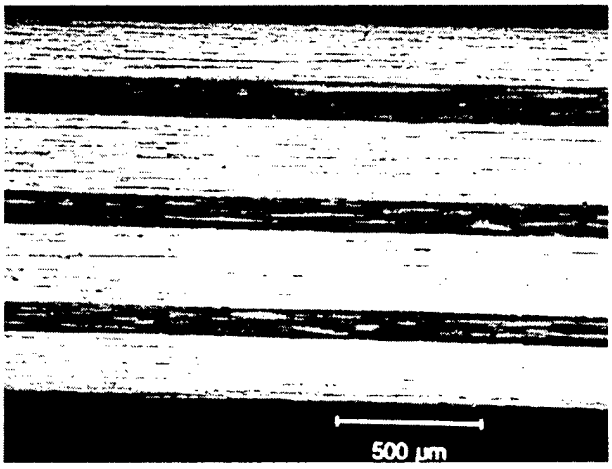

Figure 3.2 Magnification of initial HTCL cross section manufactured with 0.279 mm (11 mil) thick Ti-15-3

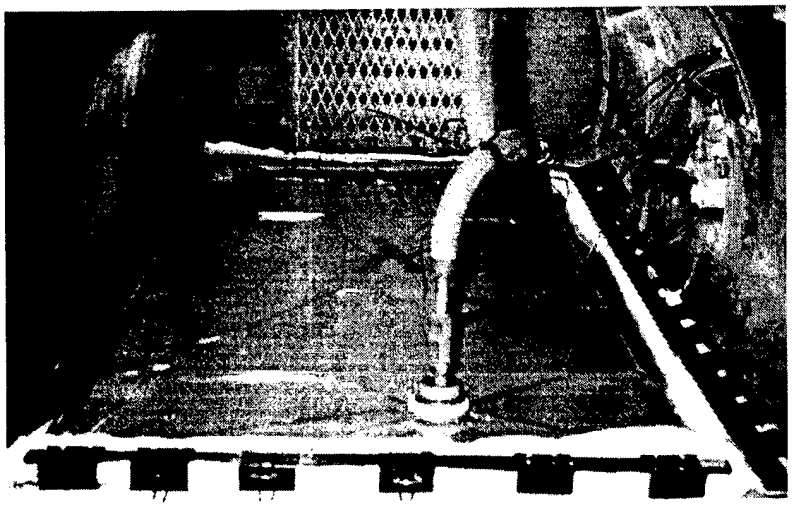

Figure 3.3 Consolidation of advanced HTCL on autoclave mold plate prior to curing

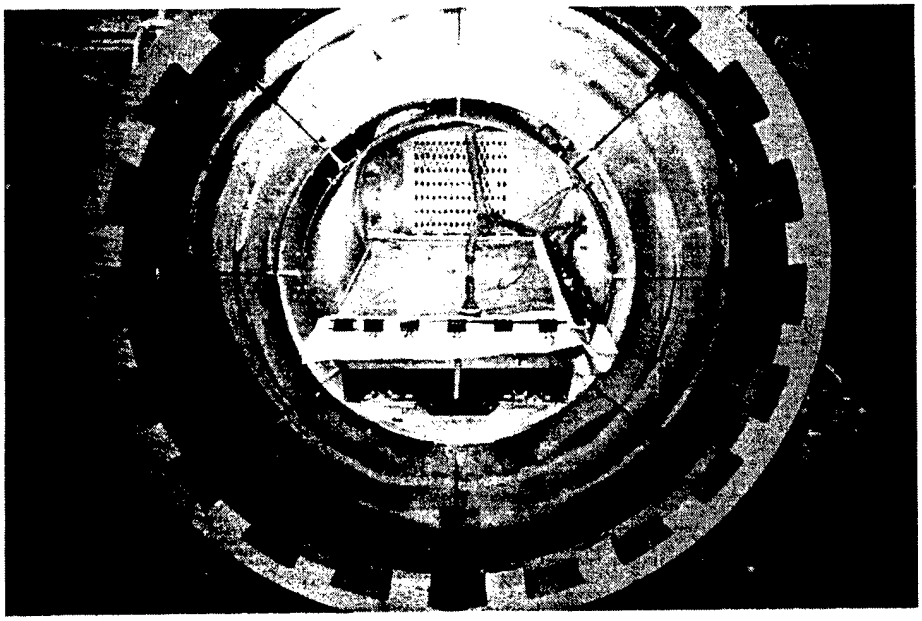

Figure 3.4 Autoclave used for curing of HTCL at NASA-Langley Research Center

CHAPTER IV

INSTRUMENTATION AND EQUIPMENT

The testing of this research was conducted in the Mechanical Properties Research Laboratory (MPRL) in the Bunger-Henry Building. In this Chapter, the test setups and equipment used in the current research are summarized. Photographs of the equipment are included in the Appendix.

4.1 Testing Setups

All tensile testing of HTCL was conducted using one of two screw-driven test frames, one with a 10 metric ton (22 kip) load cell while the other possessed a 25 metric ton (50 kip) load cell. Both used a computer controlled data acquisition system and used mechanical friction grips to secure the specimens. For constant amplitude fatigue of HTCL, one of two servo-hydraulic test machines were used. One contained a 25 kN (5.5 kip) load cell with hydraulic grips with diamond surface wedges, while the other used a 10 metric ton (22 kip) load cell and mechanical grips. Both used a computer program for control and data acquisition.

4.2 Transducers

Transducers were used for tensile testing in order to measure the stress-strain response of the HTCL. For all such tests, extensometers used a gage length of 5.08 cm (2 in). The extensometers were attached to each specimen using either steel springs, or a spring-loaded friction clip.

4.3 Microscopy

For fatigue damage analysis, a travelling microscope was used to locate the damage along each specimen edge during testing. Once damage developed, delamination was measured by taking impressions of the damaged area using acetate replicating tape, having a thickness of 0.127 mm (5 mil) and a width of 25.4 mm (1 in). The replications were viewed and recorded using an optical microscope with attached instant camera. The microscope also allowed for photography of specimen surfaces following failure.

4.4 Thermal Testing

An environmental chamber was used to determine the temperature at which residual stresses begin to form in HTCL due to the cooling following the laminate cure cycle. Though not needing the set-up for thermomechanical fatigue in this investigation,

the chamber had been mounted to a servo-hydraulic test frame. The reason the machine was used for this type of test was due to its observation window. The chamber possesses a temperature range of -155°C (-250°F) to 425°C (800°F).

CHAPTER V

TEST PROCEDURES

The investigation of advanced HTCL consisted of tensile and constant amplitude fatigue testing. The goal of the procedures is an understanding of the monotonic and cyclic mechanical properties of the advanced HTCL, with an emphasis on the fatigue damage mechanisms and progression. The specimen configuration and preparation, test matrix and test procedures are discussed in this chapter. The method of fatigue damage observation and analysis is also explained. The machining of the test specimens were conducted at the machine shop at either NASA-LaRC or the School of Mechanical Engineering. Due to the hardness of the material, carbide band saw blades were necessary for the machining.

5.1 Specimen Configuration

The specimens were cut into one of three configurations as shown in Figure 5.1. For tensile testing, both the straight-sided configuration and the dog-bone shaped specimen were used. However, for fatigue testing, only straight-sided specimens were used. In the previous HTCL research, Li [28] conducted experimentation in fatigue using both dogbone and straight-sided specimens in order to determine any mechanical

response differentiation due to specimen configuration. He determined that fatigue cracks consistently developed at the fillets of the dogbones due to the stress concentrations and that more consistent fatigue data was acquired from using straight-sided specimens. Therefore, in order to consistently monitor damage propagation without the effects of geometry, the straight-sided specimens was chosen for tension-tension fatigue tests. Shorter straight-sided specimens were used for tension-compression fatigue to avoid Euler buckling.

For all specimens, the width of the HTCL within the gage length is 12.7 mm (0.5 in). With the laminate thickness being approximately 1.47 mm (58 mil), the average cross-sectional area of each specimen is 161.3 mm^2 (0.029 in^2).

5.2 Specimen Preparation

Each HTCL specimen required careful surface preparation due to two major concerns: machining induced defects and damage observation. Particularly for fatigue, it is critical to remove the machining defects of each specimen prior to testing, therefore each specimen was sanded with 120 grit garnet paper to remove machining defects along the edges. Since the Ti-15-3 experiences high notch sensitivity, particularly in such a thin form, the removal of defects was critical. The 1.27 cm (0.5 in) surfaces of each specimen were also sanded to 120 grit, either initially with a rotary tool and eventually by hand to remove oxide that formed on the titanium surfaces as a result of the cure cycle.

This was performed for ease in observation of cracks which propagate through the outer titanium layer.

However the observation of damage initiation and propagation is through the thickness most critical, so further surface finishing at the specimen edges was necessary. The typical onset of HTCL fatigue damage is expected to begin with titanium ply cracking at the specimen edge. Therefore, each edge was polished to a finish using 4000 grit (equivalent to a grain size of 5 μm) SiC paper. The polishing was achieved in steps from 320 grit (46 μm), 500 grit (20 μm), 1200 grit (14 μm), to 2000 grit (10 μm).

To avoid failure of the specimens in the grip area, particularly for the straight-sided specimens, tabs were bonded to the specimens. The HTCL was tabbed using the same 0.254 mm (10 mil) Ti-15-3 foil used in the HTCL construction. The foil was cut to 3.18 cm (1.25 in) X 12.7 mm (0.5 in) and bonded to the specimens with adhesive film, leaving ~10.7 cm (4.2 in) of gage length for the tension-tension specimens and 2.54 cm (1 in) for the tension-compression specimens.

5.3 Test Matrix

The test matrix for all of the current research is given in Tables 5.1 through 5.3. Monotonic tensile properties of the material are always desired to characterize the overall strength of a material; however, the major concern of the current investigation is the effectiveness of the modified HTCL interface in fatigue loading. Therefore, only a few

specimens were reserved for tensile tests, while the balance of HTCL was used for fatigue testing.

For the fatigue investigation, both tension-tension and tension-compression tests were conducted in order to accurately characterize the effect of interface strength on fatigue life and damage progression. The stress levels are chosen for comparison with the data acquired in the initial HTCL investigation by Li [1]. With limited specimens of the initial HTCL available for testing and since tension-compression fatigue was not performed in the initial investigation, the two remaining initial HTCL specimens were used solely for tension-compression tests. It is important to note that all stress levels are far above that expected in the actual material application.

5.4 Test Procedures

Both tensile and fatigue tests were conducted on the advanced HTCL for comparison to the initial HTCL. The tensile testing was conducted using both straight-sided and dogbone specimens. All fatigue tests were performed using straight-sided specimens. All testing was conducted at room temperature (25°C).

5.4.1 Tensile Testing

Even though the goal of the investigation is focused on fatigue properties, the monotonic properties of advanced HTCL are also desired. The strength and stiffness of the advanced HTCL was determined by tensile tests to failure. Though HTCL specimen

geometry has a significant effect on fatigue performance, comparisons between configurations have not been conducted for tensile testing. Therefore, both straight-sided and dogbone configurations were tested for such comparison.

For tensile testing, the HTCL was tested in a mechanical screw driven test frame (either setup 1 or 2) under a displacement control of 0.254 mm (0.1 in) per minute. Straight-sided specimens were tabbed as previously mentioned due to the use of mechanical grips. The dogbone-shaped specimens, though also gripped mechanically, were not tabbed as there was sufficient material within the grip section to ensure failure occurred within the gage length.

For test setup 1, transducer 1 was for strain measurements and for setup 2, transducer 2 was used. For both extensometers, double stick tape was applied to each specimen at the point of attachment to prevent slipping. Both displacement and strain were recorded with the corresponding load. All data were acquired via the MTI Phoenix computer controller/data acquisition system.

5.4.2 Constant Amplitude Fatigue

With the goal of the current research involving the observation of fatigue damage, constant amplitude fatigue testing comprises the majority of the procedures. Fatigue testing was performed to create an experimental S-N curve and to determine the effect of incorporating a stronger PMC resin/titanium surface treatment interface into HTCL. All fatigue testing was conducted on one of two servo-hydraulic test frames (setup 3 or 4), depending upon availability. Testing was conducted using a sinusoidal cyclic waveform

in load control. Before testing, care was taken to ensure all specimens were aligned properly using a square edge along the grips. This was done so that loading was applied through the center of the specimen, thereby avoiding fatigue induced by bending.

5.4.2.1 Tension-Tension

All tension-tension fatigue testing was conducted at a stress ratio (R-ratio) of 0.1, the same ratio used in the previous research of initial HTCL [1]. The fatigue loading was imposed at a frequency of 10 Hz. Both test setup 3 (with hydraulic pressure grips) and setup 4 (with mechanical grips) were used for tension-tension testing. The cycles were recorded via the TestStar controller/data acquisition system

Configuration A was used for tension-tension fatigue testing. As mentioned previously, specimen edges were polished to a grain size equivalent of 5 μm using 4000 grit SiC paper to ensure accurate damage observation. Specimens were also marked on each face from one to seven at 1.79 cm (0.5 in) intervals to assist in locating in damage as shown in Figure 5.2.

5.4.2.2 Tension-Compression

A series of tension-compression fatigue tests was conducted to more decisively determine the effect the strengthened HTCL interface has on fatigue damage progression once a titanium ply crack was initiated. Tension-compression tests were conducted on the initial as well as advanced HTCL in the current investigation.

Tension-compression testing was conducted with an R-ratio of –0.2. The same care was taken to ensure specimen alignment, particularly as the potential to induce specimen bending is higher under compressive loads. The frequency of the fatigue cycles was slowed to 5 Hz with the potential for a much more unstable failure mode at the onset of initial damage. Since the teeth of the mechanical grips in test setup 4 are oriented to be most conducive for tension-dominated tests, setup 3 with hydraulic pressure grips was employed for all tension-compression testing. A mechanical stop was attached to the servo-hydraulic actuator to prevent complete specimen destruction in the event of failure in compression.

All specimens were straight-sided and with only a 2.54 cm (1 in) gage section (See Figure 5.1), and only three markings were made on each face at 1.79 cm (0.5 in) intervals as shown in Figure 5.3 to assist in damage documentation. Again, specimen edges were polished to observe damage initiation and progression.

5.4.2.3 Fatigue Damage Observation Methods

For both tension-tension and tension-compression testing, the fatigue stress-life approach was used by reporting specimen failure for each stress level and an S-N curve was thereby developed for comparison to the initial HTCL research. However, to adequately determine the effect the strengthening of the interlaminar interface, more detailed investigation was necessary. This investigation was manifested in three distinct forms: the number of cycles until damage initiation, the damage progression, and interface surface inspection at failure.

The initiation of fatigue damage was easily performed by logging the number of cycles until a visible macroscopic crack develops in the HTCL. Based on previous HTCL research such damage is expected to occur at the titanium ply edges, therefore, observing the thin edges of the HTCL were necessary [1]. Since each specimen edge was highly polished, damage initiation could be observed by the naked eye with sufficient lighting. Damage could initiate on either side, so test setup 3 was used for fatigue damage monitoring as both the front and back edges of the specimen could easily be accessed. Once a titanium ply crack was suspected to form, an optical microscope was used to inspect the damage for verification.

The progression of damage, following crack initiation, was then recorded for each fatigue test. In particular, the prospect of titanium ply delamination is expected of chief concern. Therefore, at the onset of a titanium ply crack, further HTCL damage was recorded via plastic tape replication of the specimen edges. For successful replication, the fatigue cycle was recorded and manually paused to halt the specimen motion. The replicating tape used was cellulose acetate tape with a thickness of 0.127 mm (5 mil). Acetone was applied to the surface and the plastic tape was immediately pressed onto the damaged region with a lead eraser and held for ~30 seconds. The replication was taped to a glass microscope slide. Damage was then observed via an optical microscope. This procedure was repeated to record damage progressing with the fatigue cycles following titanium ply cracking.

The microscope was also used for the inspection of surfaces and interfaces after specimen failure. All replicates and specimen surfaces were photographed via the microscope for data presentation.

Table 5.1 Tensile test matrix for advanced HTCL

SPECIMEN CONFIGURATION	NO. OF TESTS
Straight-sided (long)	2
Dogbone	2

Table 5.2 Constant amplitude fatigue test matrix for tension-tension loading (R = 0.1) using advanced HTCL

APPLIED MAXIMUM STRESS MPa (ksi)	NO. OF TESTS
682.6 (99.0)	1
696.4 (101.0)	1
703.3 (102.0)	1
710.9 (103.1)	2
730.9 (106.0)	1
750.9 (108.9)	2
790.2 (114.6)	1
827.4 (120.0)	3
869.5 (126.1)	3

Table 5.3 Constant amplitude fatigue test matrix for tension-compression loading (R = -0.2)

APPLIED MAXIMUM STRESS MPa (ksi)	NO. OF TESTS
Advanced HTCL	
551.6 (80.0)	1
655.0 (95.0)	1
724.0 (105.0)	1
758.5 (110.0)	1
786.1 (114.0)	1
827.4 (120.0)	1
868.8 (126.0)	1
Initial HTCL	
655.0 (95.0)	1
786.1 (114.0)	1
827.4 (120.0)	1

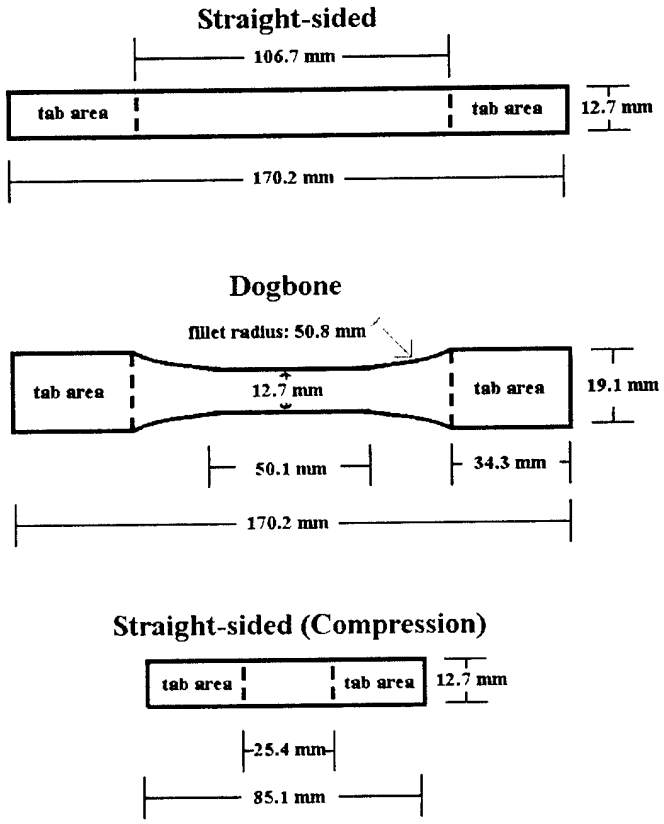

Figure 5.1 Specimen configurations for advanced HTCL mechanical testing

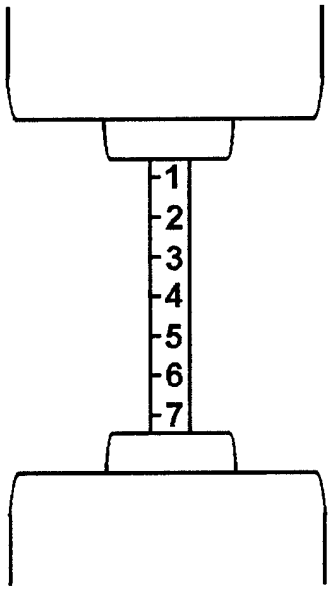

Figure 5.2 Specimen marking to document damage location for tension-tension fatigue testing

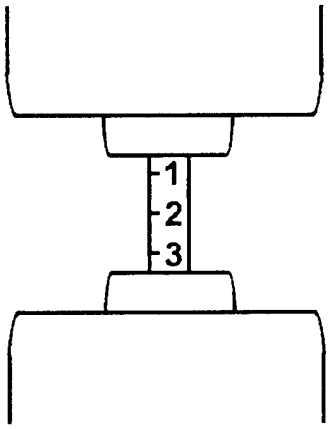

Figure 5.3 Specimen marking to document damage location for tension-compression fatigue testing

CHAPTER VI

RESULTS AND DISCUSSION

The experimental results for the testing of advanced HTCL are presented in this chapter. First, the residual tensile stresses are presented and discussed. Both the tensile and fatigue results of the advanced HTCL will be compared to the initial HTCL data of Li [1]. The monotonic properties of the advanced HTCL will be presented initially with an AGLPLY comparison, followed by the results of the series of fatigue tests. The fatigue damage initiation, progression, and ultimate specimen failure surfaces will be discussed and compared for each HTCL construction.

6.1 Residual Stresses

Before presentation of the experimental results, it is appropriate to determine the residual stresses of the HTCL. Residual stresses exist in the laminate due to the differences in coefficients of thermal expansion (α) of the constituents [29]. Due to these differences, the stresses are induced in the constituents as the laminate is cooled during the curing process. Values of α for Ti-15-3 and the IM7 fibers are available from their respective manufacturers, while the value for the PETI-5/IM7 PMC prepreg was obtained from P. Hergenrother [30] at NASA-LaRC. A value of α for PETI-5 alone was not

readily available. However, with the known values of α_{pmc}, V_f, and α_{IM7}, α_{PETI-5} could easily be calculated using rule of mixtures. All values for α are found in Table 6.1.

The values for residual stresses in each lamina were calculated using a thermomechanical composite prediction code called AGLPLY. Bahei-El-Din [31] developed the AGLPLY program (originally for metal matrix composites) to predict the elastic-plastic response of composite laminates and their constituents due to thermal and mechanical loading using the properties of the constituent materials and the rule of mixtures. For the residual stress calculations, the laminate was given only a thermal load, beginning with a maximum temperature of 265°C (509°F) from the cure cycle and finishing at room temperature.

Though the cure cycle actually reached a height of 371°C (700°F), residual stresses do not begin to develop until 265°C. In order to determine this temperature, a 2 ply panel, comprised of one Ti-15-3 ply on top of one PMC ply, was cured with the test specimens during fabrication. Since it is nonsymmetric, the laminate curled into a "U" shape as a result of the α differential, with the Ti-15-3 on the upper surface and the PMC on the lower surface contracting and expanding, respectively, as it cooled from the cure cycle. With each end deflected 39.7 mm (1.56 in), the laminate was placed in an environmental chamber and heated so the ends would begin to fall as the plies began to either expand/contract back to the original flat shape at cure. At 265°C, the ends ceased to move, indicating the temperature at which residual stresses are induced when a symmetric laminate is cured. The results for this test are illustrated in the graph in Figure 6.1. Note that the ends did not deflect the full 39.7 mm to return to a flat position as the

initial Ti-15-3 foil alone possessed some residual curl obtained in manufacturing and rolling. It was at this level of deflection that the laminate ends ceased to fall in the test.

The results of these residual stresses calculations in the titanium and PMC layers are presented in Table 6.2. As seen in the previous research [1], there exists a residual tensile stress in the titanium as it desires to contract during cooling as it has a positive α. Meanwhile the PMC layer, with a negative α, wants to contract, and therefore compressive residual stresses are induced.

6.2 Tensile Testing

The following sections discuss the results of several monotonic tests of HTCL and are validated in the comparisons to previous HTCL data as well as results from a proven prediction code. The mechanical properties of advanced HTCL are listed in Table 6.3 and are illustrated via stress-strain curves in Figures 6.2, 6.3, and 6.4. The yield strength of all HTCL is approximated using the proportional limit corresponding to the knee in each curve. The knee of each curve indicates initiation of titanium ply yielding, since the PMC plies behave in a brittle nature.

6.2.1 Configuration Comparison

Experimental results were obtained by conducting tests of the straight-sided vs. dogbone specimens to determine which behaves with more consistency. Table 6.3 and Figure 6.2 show that the straight-sided specimens had a slightly higher modulus while

possessing a lower ultimate strength. However, there was more significant variance in the data amongst the straight-sided specimens than in the dogbones. Each dogbone behaved almost identically in stiffness and yield stress. An explanation for this result is due to the consistent nature by which the dogbone geometry inherently ensures more consistent material strain within the gage section. Moreover, each straight-sided specimen failed near the grip section while the dogbones consistently failed within the gage section. Though previous configuration testing by Li [28] showed straight-sided specimens prove more reliable than dogbones in fatigue, the opposite trend is observed in tensile testing.

6.2.2 AGLPLY Comparison

To further validate the experimental results, the mechanical response of HTCL was predicted using AGLPLY analysis. The AGLPLY stress-strain computer code was used extensively in previous HTCL analysis and was shown to compare favorably with the experimental tensile data [15, 32].

Figure 6.3 illustrates the comparison between AGLPLY and the average stress-strain response for each specimen configuration. It is clear the dogbone specimens produce a very similar mechanical response to the AGLPLY prediction, particularly in the elastic region. The respective moduli compare very favorably as shown in Table 6.3, however AGLPLY overestimates the plastic response of HTCL. This same trend was observed by Li et al [32] in an extensive AGLPLY parametric study conducted in the previous analysis. Possible sources for error include variations in the actual fiber volume

fraction in the experimental that differ from the predicted value used in AGLPLY. AGLPLY also incorporates the vanishing fiber model and does not incorporate micromechanical effects and damage. The program also is susceptible to error when the fiber direction is not aligned with loading, however such was not the case for this HTCL.

6.2.3 Initial HTCL Comparison

Figure 6.4 compares the initial HTCL tensile results with the advanced HTCL data. In light of the specimen configuration results, the advanced HTCL curve only incorporates the experimental results using the dogbone specimens. The tensile strength values compare well since they are driven by the properties of the IM7 fibers, which are the same for each laminate. Similarly, there is little difference in the yield strength of the two laminates. However, the advanced laminate possesses a slightly higher modulus than that of the initial HTCL.

The major cause of this higher stiffness can be attributed to the difference in titanium ply thicknesses between the two laminates. Recall that the initial HTCL was constructed with 0.279 mm (11 mil) thick Ti-15-3 foil, while the advanced HTCL possesses 0.254 mm (10 mil) foil. With 11 mil foil, the initial laminate possesses a volume fraction of PMC plies of 0.25 while the titanium being 0.75. In the advanced laminate, the PMC volume fraction is approximately 0.28 and the titanium is 0.72. With a greater percentage of the much stiffer PMC carrying the laminate load, an increase in modulus is expected. This has been proven using the rule of mixtures which has shown to be effective in mechanical property predictions for hybrid composite laminates [33].

Accounting for this and experimental variability, there is little to no difference in tensile properties of between the advanced and initial HTCL. Consequently, there is no impact on the monotonic behavior of HTCL due to interface strength, as one might expect.

6.3 Constant Amplitude Fatigue

The experimental results for constant amplitude fatigue, including fatigue life and damage progression, are presented with respect to the effects of mean stress on the advanced HTCL. Therefore, the results of both tension-tension and tension-compression fatigue will be discussed, beginning with the overall fatigue life followed by a more detailed discussion of the initiation of damage, its subsequent progression, and finally the results of investigating specimen failure.

6.3.1 Tension-Tension

The HTCL was fatigued until specimen failure the same stress levels the initial HTCL was previously tested shown in Table 5.1 [1]. All tension-tension tests were conducted with a stress ratio (R) of 0.1 at a frequency of 10 Hz. The specimens were considered failed when they could no longer carry any fatigue load. The number of cycles to failure at each stress level was used to produce an S-N curve. Figure 6.5 illustrates the fatigue life for advanced HTCL as compared to initial HTCL. The S-N curves show a similar slope, however the advanced HTCL curve shows higher life with

an increase in the endurance limit from 730.8 MPa (106 ksi) to 751.6 MPa (109 ksi). One possible reason for such improvement may again be a result of the differences between the volume fractions of the constituents between advanced HTCL and the initial HTCL, as in the case of tensile testing. Just as in monotonic tests, the fatigue loads applied to HTCL are dominantly carried by the much stiffer PMC layer. Therefore, a variation in the percentage of each may alter the fatigue life. Yet this increase in fatigue life and endurance limit is not statistically significant, given scatter and experimental variability.

In order to better understand the effects of the constituent properties and determine which lamina was the limiting material, Li [1] developed a qualitative illustration of the load carrying capabilities of the HTCL constituent plies. He plotted the proportional stresses carried in both the titanium and PMC plies with respect to the actual HTCL S-N curve, based on the respective ply moduli. As a result, he showed the titanium carries a lower stress as compared to the laminate while the PMC layers carry a higher stress. A similar graph for advanced HTCL is shown in Figure 6.6 accounting for the residual stresses in each ply. Though noting this representation only designed to indicate the trend of fatigue stress levels amongst the laminae, Li [1] went on to show the experimental fatigue life for monolithic Ti-15-3 very closely approximates the proportional titanium S-N trendline, proving the HTCL fatigue life is chiefly limited by the fatigue life of the titanium plies.

6.3.1.1 Fatigue Damage Initiation

As expected, the first visible fatigue damage occurs with a crack initiating in a titanium ply. The cracks consistently initiate at one edge and propagate through the entire ply width, a trend Johnson [10] observed in fatiguing adhesively laminated titanium. At the outset of fatigue testing a majority of these cracks initiated in one of the outer titanium plies, as observed in Li's [1] investigation. However, with a different sanding method used to remove the oxide layer from the faces of the outer plies, a few initial cracks of the titanium began appearing in one of the two inner plies. The reason for such a change in initial cracking location due to sanding may lie in the greater potential for crack initiation due to surface defects.

As mentioned previously, Ti-15-3, like most titanium alloys, is extremely notch sensitive and significant care was taken to ensure machining defects were kept to a minimum along the edges. However, such care was not initially taken on the larger outer HTCL titanium faces to remove the dark oxide developed during curing. Recall that the surfaces were sanded using 120 grit paper via a rotary tool and by hand. Though the same grit was used, the action of the rotary tool produced far more surface defects and thereby causing premature cracking in the outer titanium. Figures 6.7 and 6.8 show comparisons of the two different specimen surfaces. Moreover, many rotary tool sanded specimens produced significant multiple cracking, with up to five cracks along the same ply prior to failure for some specimens. As a result, cracks initiated much sooner and the fatigue life was much shorter for those prepared with the rotary tool as shown in Figure 6.9. These results show importance of proper surface preparation for fatigue of titanium.

Given the proper preparation for the HTCL outer surfaces, more confidence could be placed in the number of cycles until the initial crack as well as any trend in its location. Figure 6.10 illustrates the HTCL comparison of onset of the initial titanium ply crack and specimen failure. For more ease in comparison, Table 6.4 shows the number of cycles from initial titanium cracking to ultimate specimen failure. From these results, it is clear that the advanced HTCL shows a substantial increase in cycles-to-failure following damage initiation over the initial HTCL for identical stress levels. In HCF, the difference is an order of magnitude. Therefore, given titanium ply cracking occurs at the same cycle count for each stress level, the advanced HTCL would maintain a higher, improved S-N curve. This indicates the interfacial strengthening did increase the fatigue life following damage. The application of this improvement can be realized in component inspection intervals following reported damage. With more time between damage initiation and material failure, inspection intervals can be reasonably developed.

6.3.1.2 Fatigue Damage Progression

Tension-tension damage propagation following initial titanium cracking was observed for the advanced HTCL, but was not previously accomplished for initial HTCL. The damage was closely monitored to observe any effects of the strengthened interface, specifically the advent of titanium ply delamination due to Mode I/Mode II (mixed mode) type loading. To do so, the fatigue cycle was stopped once a titanium crack was observed and plastic replications were taken of the edge of the specimen at the area of this crack. As mentioned, some of the initial cracks occurred in one of the inner titanium plies,

which was a different trend from the initial HTCL investigation. To show the effects in advanced HTCL of both an inner titanium ply and an outer titanium ply initiating first, the damage progression will be presented for each case.

A case with an inner ply titanium crack initiating first is shown in Figure 6.11 and occurred at 100,000 cycles in a specimen tested with a maximum stress level of 869 MPa (126 ksi). The crack has already propagated to the other edge. A replication was taken of this cracked region on both the front and back edges at this cycle and every 5,000 cycles following until specimen failure. These replications were viewed under the microscope to determine the extent of the damage for each number of cycles. Figures 6.12 through 6.21 show the replication photographs of both sides and their respective schematics showing the magnitude and direction of damage progression as the cycles accumulate. These magnitudes of the damage lines in the schematics are not drawn to scale, however their lengths are reported with dimensions of μm. The (+) sign shown in Figure 6.21 indicate the damage propagated at least to the magnitude reported beyond as it progressed beyond the area of the replication.

Two important observations can be made from these Figures. First, the schematics show the some of the damage to propagate along the interface but some damage, though still mostly following a path in the longitudinal direction, begins to propagate into the PMC layers. Though difficult to see in each replicate photograph, such a trend was validated by observation of the final failure surface that shows fibers remaining bonded this inner titanium ply. The second observation (depicted in Figures

6.18 through 6.21) is the initiation of a second crack in the adjacent outer titanium ply and its subsequent failure occurring only 600 μm away from the initial crack.

The first observation is a direct result of a strengthened interface. Recall that a cracked titanium ply in the initial HTCL consistently delaminated along the length of the specimen at the interface. The advanced HTCL possesses a strong enough interface to prevent interfacial delamination, such that a stress concentration breaks the fibers still bonded to the cracked titanium. This trend is better observed, as it does so to a greater magnitude, when an outer titanium ply cracks. Figure 6.18 is the first image of the previous series showing the outer ply cracked. Fibers are visibly bonded to the titanium ply along its length. In a case where the outer titanium ply cracks first, this phenomenon occurs to an even greater degree. Figure 6.22 shows a replication of an outer ply titanium crack formed at 37,000 cycles in a specimen fatigued at a maximum stress of 120 ksi. This figure shows close to half of the thickness of the adjacent PMC layer has cracked and has remained bonded to the damaged titanium layer. In both cases, there is a limit to the amount of PMC that cracks adjacent to the titanium. In no test was a titanium fatigue crack observed to propagate through the entire adjacent PMC layer, but eventually always progressed longitudinally in between the fibers in a manner that effectually delaminated the ply as a result of predominantly Mode II loading.

It is important to note that the first observation only characterized one of two typical scenarios resulting from a failed titanium ply. While often no interfacial delamination was produced between the titanium and PMC layers, in many cases, delamination did occur. However, such delamination always eventually propagated from

the interface to the PMC layer, such that most of the length of the failed titanium ply remained bonded to some layers of fiber. This trend is discussed in more detail in the following section as failure surface inspection sheds significant light on this finding.

The second observation (the longitudinal proximity of the second titanium ply cracking in relation to the first) is not the result of a strengthened interface, however this deduction can't be made with the same level of certainty due to variability in the results. As just observed, the first example produced a second crack 600 μm away from the first. In the second example previously mentioned, the outerply damage was followed by the opposite outer titanium ply cracking, this time 50,000 μm (~0.25 in) in longitudinal distance away. However in other tests, the second titanium ply damage often occurred at the opposite end of the specimen. The strength of the interface can have an effect on such progression in laminates such as HTCL. As mentioned in Chapter 2, Marissen [18] showed that given an overly strong interface and perfect fiber-bridging scenario, a cracked metal layer would produce an infinite stress concentration in the adjacent fibers resulting in a crack that "zips" through and catastrophically fails a hybrid composite laminate. However, as just mentioned, the broken fibers in the PMC layer adjacent to the titanium never propagate the entire lamina thickness due to Mode I loading, but eventually propagate longitudinally between the fibers of this layer dominated by Mode II loading. Furthermore, the third and last remaining titanium plies for the above mentioned examples cracked at a significant distance away from the initial two ply cracks. Figures 6.23 and 6.24 illustrate this damage progression for each respective example. What can be stated is that the second (and often times all subsequent) titanium

ply cracking typically forms within the distance of effectual delamination between the fibers caused due to the initial titanium ply damage. This is logical as the plies that have failed obviously cease to carry the load for the laminate as far as it is delaminated, which results in an increase in stress for the plies that remain intact within that region.

6.3.1.3 Failure Surface Inspection

As mentioned in the previous section, observing the failure surfaces of the HTCL plies proved beneficial in helping to retrace the evolution of damage. This proved most effective in the event of delamination occurring at the interface in the presence of a cracked titanium ply. Recall from the schematics of Figures 6.12 through 6.21 that damage appeared to progress at the interface for one side of the failed ply. Though this appearance proved accurate for at least the area of the specimen covered by the tape replication, inspection of this surface following specimen failure proved this delamination to propagate at the interface for a limited length along the specimen. Eventually, the delamination propagated between the fiber layers. Figure 6.25 is a photograph of the bottom section of this ply showing the surface experiencing the most apparent interfacial delamination as viewed via replication. It is clear however, that in light of the amount bare titanium resulting from this delamination only progressed a limited distance before travelling between the fibers. Furthermore, the delamination throughout this distance did not propagate across the entire specimen, but is only evident at the edges.

With further failure surface inspection, this limited delamination proved particularly common for inner titanium ply failure. Whether the first or second ply to fail, the inner plies produced far more interfacial delamination than did outer plies. While Figure 6.25 proved a typical inner ply fatigue surface, Figure 6.26 was representative of outer ply damage. This figure is a photograph of the surface of the lower outer titanium ply which failed at 115,000 cycles as viewed in Figure 6.18. It is clear that the fibers remaining bonded to almost the entire titanium surface.

One possible explanation for this is due to a difference in the type of loading induced in each scenario. When an outer titanium ply cracks and fails, the resultant loading condition is not purely a Mode II type, but is actually a mixed-mode situation with mostly Mode II, but some Mode I type loading as well as it forms what is, effectively, two cracked lap shear (CLS) specimens. However, when an inner ply cracks, this mixed-mode loading does not occur as the delaminating ply is not "peeling away" from the adjacent plies. Since the interface optimization testing previously performed by Cobb [2] used for the current research was conducted using CLS specimens, we might expect a greater success in the bonds which see the mixed-mode loading over strictly Mode II behavior.

6.3.2 Tension-Compression

Figure 6.27 shows an S-N curve for the advanced HTCL, using an R-ratio of –0.2 and is graphed in comparison to the tension-tension curve constructed. A slight decrease in fatigue life is shown for the tension-compression. This is a result of the substantial

increased stress range. Though the S-N curve shows a somewhat disproportional drop in life at high cycle fatigue, indicated by the change in slope from the R = 0.1 curve to the R = -0.2 curve, it should be noted that considerable scatter is expected at HCF. The same trend was observed in Figure 6.28 for the initial HTCL comparison. In comparing, the initial to the advanced laminate in tension-compression, the S-N curve shows the initial HTCL to actually possess a slight increase in fatigue life in Figure 6.29. (Note that only two initial HTCL specimens were available for the tension-compression testing, with one tested a second time after being tested at 655 MPa (95 ksi) to runout with no damage.)

6.3.2.1 Fatigue Damage Initiation

As in the case of tension-tension fatigue, damage initiated with titanium ply cracking and subsequent propagation across the ply width. Though still the majority of the initial plies to crack were outer plies, inner ply damage occurred initially on a few occasions, as in the case for R = 0.1 loading. In either case, titanium ply cracking occurred substantially sooner in tension-compression fatigue for advanced HTCL, particularly in HCF. This can be observed in Figure 6.30, comparing the initial titanium crack and specimen failure for both loading conditions. Thus some of the decrease in fatigue life is a result of the earlier initiation of titanium ply cracks while the other factor is due to a shorter life following initial cracking. Therefore, the advent of compression stresses die result in a more rapid damage progression leading to failure for the advanced HTCL.

The initial HTCL showed a more substantial drop in fatigue life following initial damage in tension-compression loading from tension-tension then the advanced HTCL. Table 6.5 compares the specimen fatigue life remaining following initial titanium cracking for both laminates at S_{max} = 786 MPa (114 ksi), R = -0.2. While the advanced HTCL continues fatiguing for 8,000 cycles following initial titanium cracking, the initial HTCL only cycles 1,468. This particular initial HTCL specimen was monitored extensively for damage progression and will be further discussed in the following section, however this result even further discriminates the effects of the interface between the laminates. The advanced HTCL increase in fatigue life of following damage validates the observation made between the laminates in tension-tension loading that the strengthened interface does increase the laminates damage tolerance.

6.3.2.2 Fatigue Damage Progression

Figures 6.31 to 6.36, typical damage propagation is shown for tension-compression testing. The damage is shown for a specimen tested with an S_{max} of 655 MPa (95 ksi) tested at R = -0.2 until failure at 122,000 cycles. Damage measurements were made via tape replication, as before. The damage progression is markedly similar to tension-tension damage progression, with outer titanium ply cracking resulting in adjacent PMC damage and subsequent effectual delamination. Similarly, inner titanium ply damage results in delamination at the interface, at least for a certain distance. Though initial titanium ply damage, and therefore ultimate specimen failure, occurred much sooner in tension-compression, similar damage propagation resulted. No significant

differences in the progression of damage were evident, nor any indication that the interfacial strengthening observed in tension-tension was lacking in tension compression fatigue.

The damage progression to failure of initial HTCL is shown for an S_{max} of 786 MPa (114 ksi) at R = -0.2 in Figures 6.37 through 6.41, recorded again via replication. Beginning with an inner titanium ply crack having cracked through the ply width at 141,000 cycles, the damage propagates very rapidly and at the Ti/PMC interface. Once the delamination moved beyond the longitudinal midpoint of the specimen, local ply buckling begin in the outer two plies with each compressive load, shown in Figure 6.39. After only 90 cycles, the opposite two plies began experiencing the same effect as depicted in Figure 6.40. Failure quickly followed 30 cycles later, illustrated in Figure 6.41. While local buckling was extremely rare in the advanced HTCL, when it did occur, in did so with separation between fibers layers, not at the interface. Furthermore, this buckling phenomenon was never observed. Again, such differences in the laminates are directly attributable to interface strength. As expected, the effect of the Ti/PMC interface strength is most evident under compressive loads once damage has begun.

6.3.2.3 Failure Surface Inspection

As Figures 6.42 and 6.43 show, a significant difference in failure surfaces exists between initial and advanced HTCL. The photo in Figure 6.42 depicts fibers bonded over a significant length of specimen following tension-compression fatigue to failure. The surface shown is an inner titanium ply and, as typical of tension-tension surfaces,

damage began at the interface and propagated to the PMC layer. Figure 6.43 shows little to no fiber adhesion and thus a mostly bare titanium surface. With failure occurring close to the grip section in this specimen, it is difficult to discern the degree of damage that occurred before rapid delamination at failure. However, such a stark contrast in titanium ply surfaces at failure further validates the significant difference in interface strength concluded in the previous two sections.

Furthermore, as was observed in the failure surface analysis of the advanced HTCL following tension-tension loading, the tension-compression failure surfaces indicate a disparity between the amount of interfacial delamination that occurs at the edge as compared to the center of the advanced specimens. The right edge of the specimen in Figure 6.42 reveals significant fibers bonded along the whole length, which is not characteristic of the rest of the specimen. Such findings further demonstrate the importance of failure surface observation in the damage progression analysis, particularly when edge surface replication is employed. Even measuring the damage at both edges does not characterize the amount of delamination that may occur towards the center of each laminate.

Table 6.1 Coefficients of thermal expansion for advanced HTCL constituent materials

MATERIAL	α μin/in °C (μin/in °F)
Ti-15-3	0.821 (0.456)
PMC (PETI-5/IM7)	-0.342 (-0.19)
PETI-5 (5000g/mol)	65.4 (36.3)
IM7 fibers	-0.396 (-0.22)

Table 6.2 Residual stresses in lamina plies for HTCL specimens at room temperature due to an autoclave processing temperature of 265°C (509°F)

LAMINA MATERIAL	RESIDUAL STRESS MPa (ksi)
Ti-15-3	78.28 (11.35)
PMC (PETI-5/IM7)	-200.09 (-29.02)

Table 6.3 Monotonic mechanical properties for advanced and initial HTCL

		E GPa (Msi)	**S_Y MPa (ksi)**	**S_{ULT} MPa (ksi)**
Advanced HTCL				
Experimental	Straight Sided	133.8 (19.4)	1177.0 (170.7)	1546.5 (224.3)
	Dogbone	120.0 (17.4)	1175.6 (170.5)	1614.1 (234.1)
AGLPLY		117.2 (17.0)	1172.1 (170)	1843.0 (267.3)
Initial HTCL				
Experimental		116.9 (16.96)	1227.3 (178.0)	1544.5 (224.0)

Table 6.4 Number of cycles remaining in initial and advanced HTCL following initial titanium ply failure for tension-tension fatigue (R = 0.1)

S_{max} (ksi)	CYCLES BETWEEN FIRST CRACK AND FAILURE	
	INITIAL HTCL	**ADVANCED HTCL**
126.1	9,000	19,682
120	NA	21,345
114.6	11,000	110,321
108.9	13,000	NA

NA (Not acquired)

Table 6.5 Number of cycles remaining in initial and advanced HTCL following initial titanium ply failure for tension-compression fatigue

S_{max} (ksi)	CYCLES BETWEEN FIRST CRACK AND FAILURE	
	INITIAL HTCL	**ADVANCED HTCL**
120	NA	16,700
114.6	1,468	8,000

NA (Not acquired)

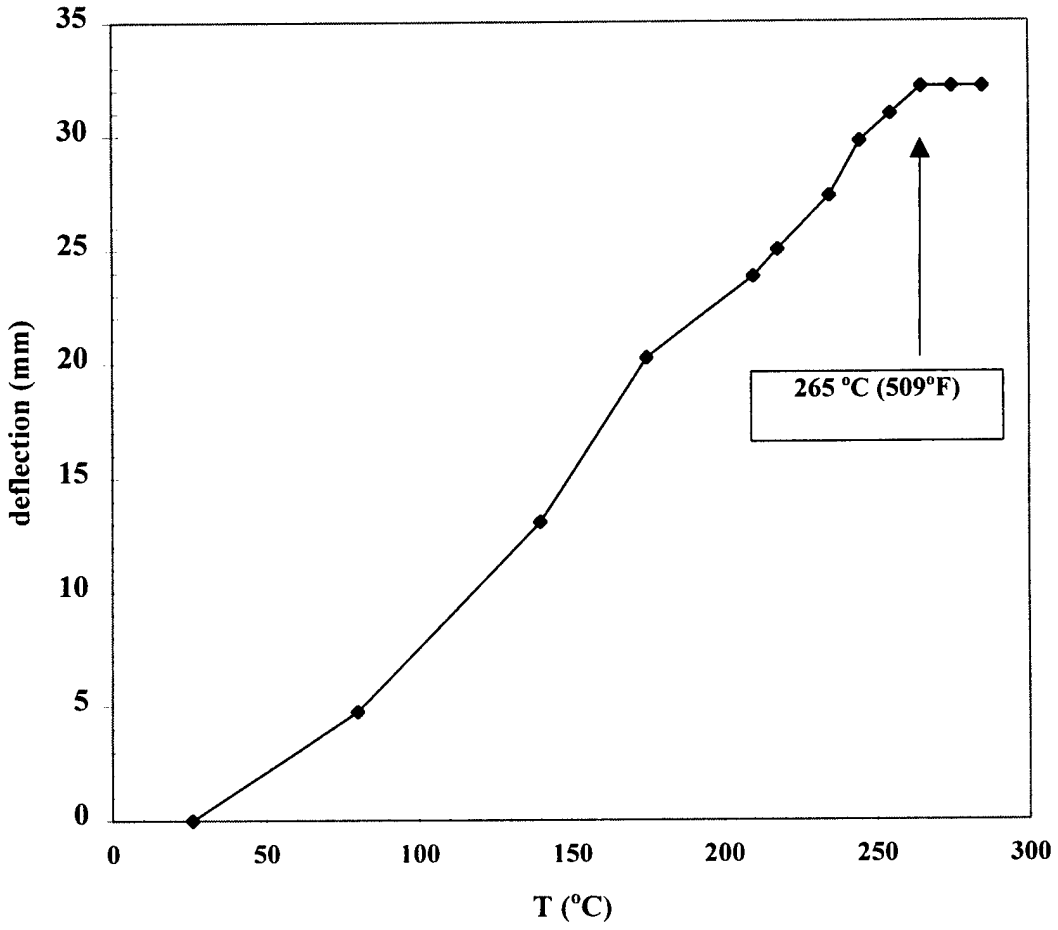

Figure 6.1 Results of two-ply HTCL for determination of temperature at which residual stresses are induced in the lamina

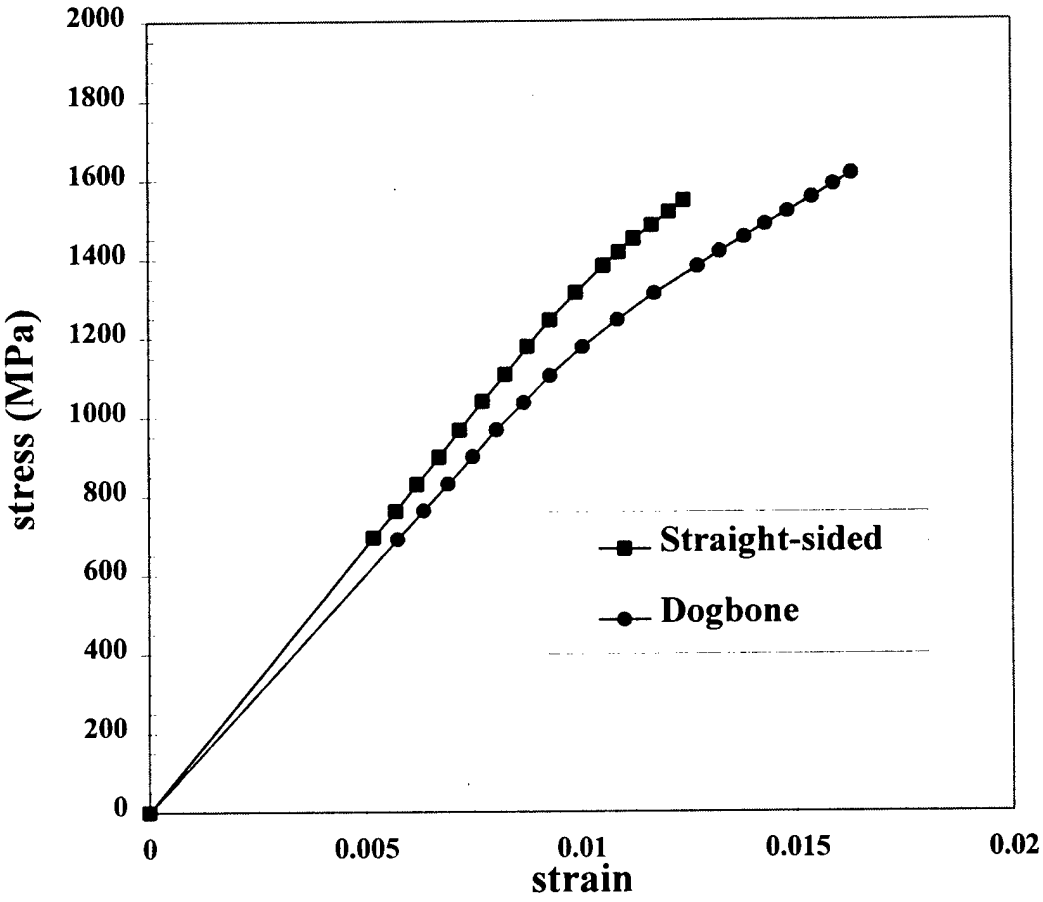

Figure 6.2 Average tensile results for advanced HTCL configuration testing

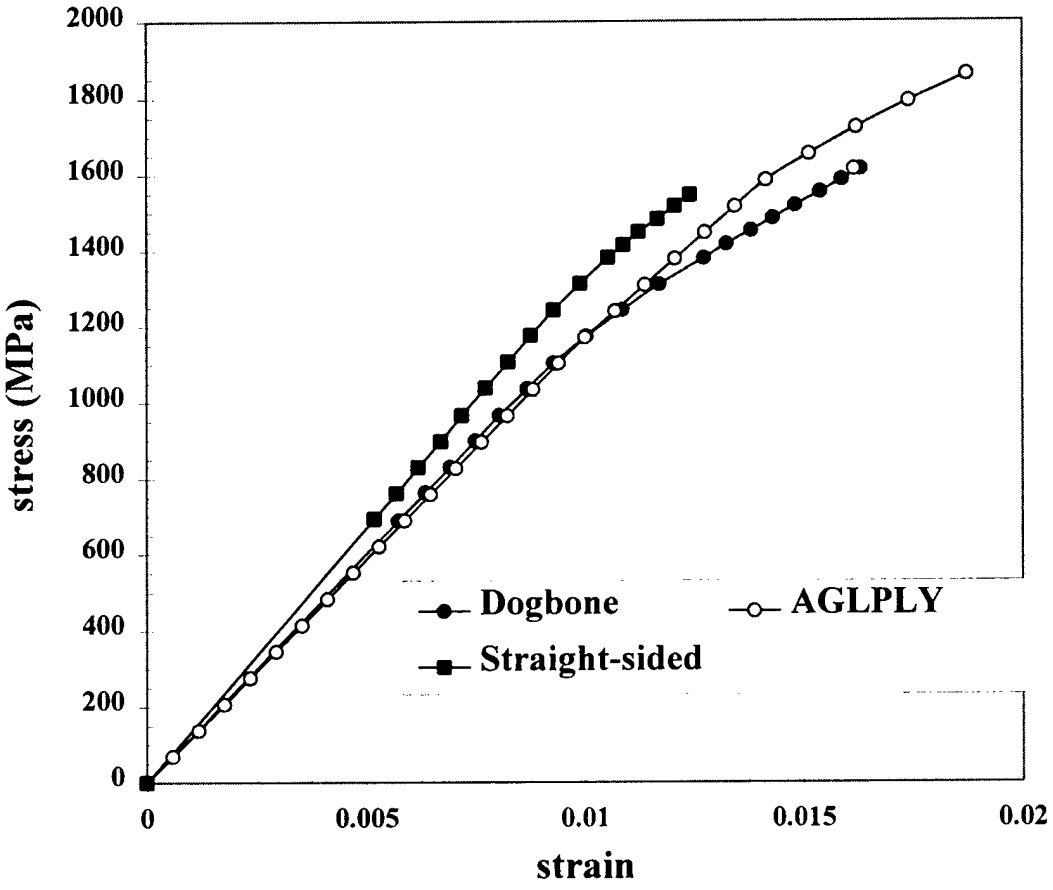

Figure 6.3 Correlation between AGLPLY prediction and both dogbone and straight-sided configuration tensile test results

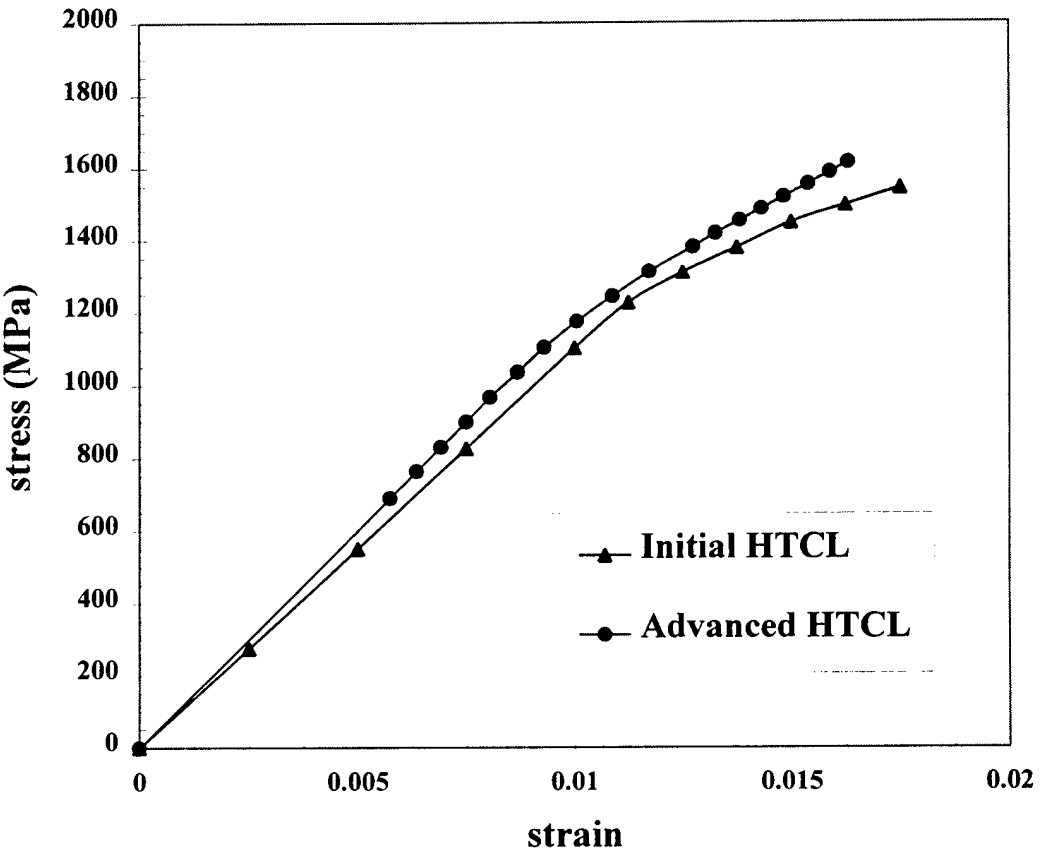

Figure 6.4 Experimental tensile test comparison of advanced HTCL and initial HTCL (Note: The initial HTCL was constructed with 11 mil (.279 mm) thick Ti-15-3 foil, resulting in a V_{PMC} of 0.25 and V_{Ti} of 0.75. The advanced HTCL possesses 10 mil (.254 mm) foil, resulting in a V_{PMC} of 0.28 and V_{Ti} of 0.72.)

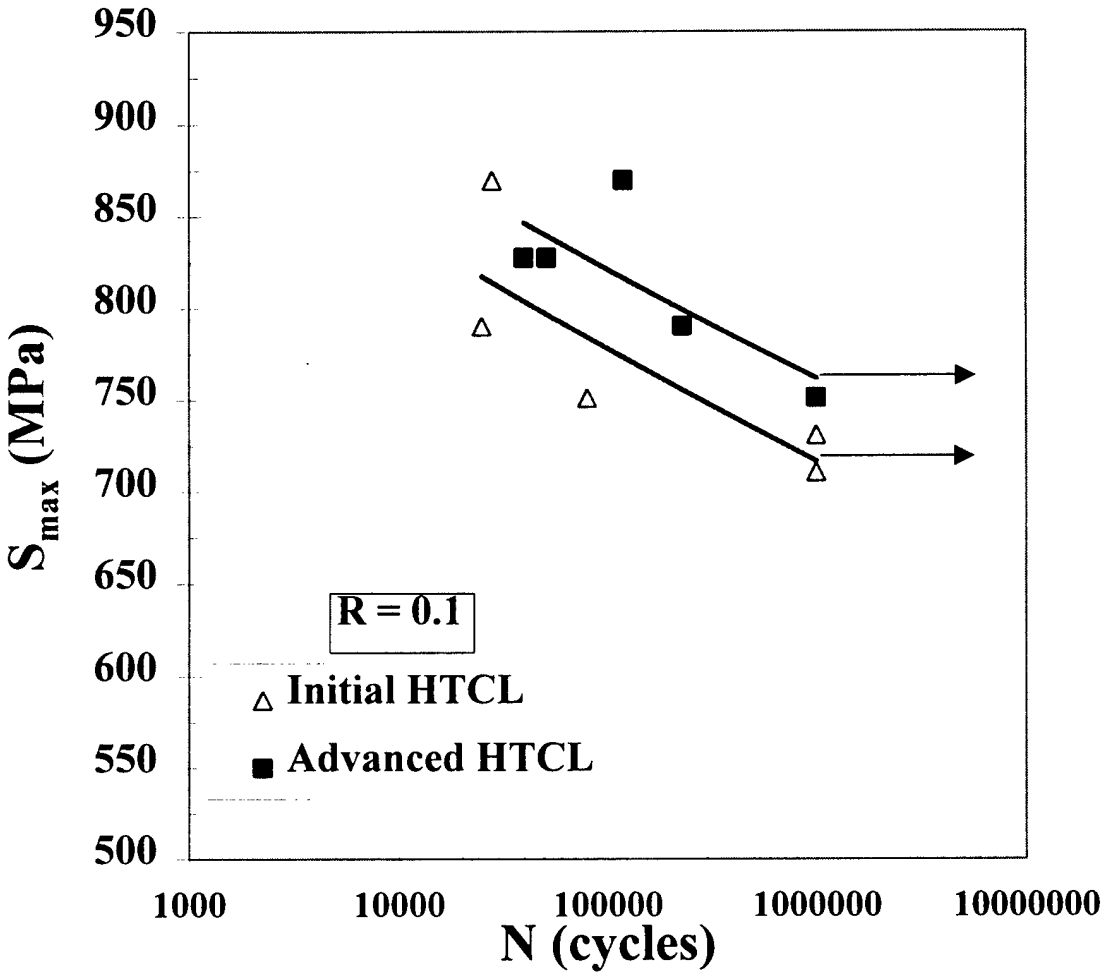

Figure 6.5 S-N curve comparison between fatigue of initial and advanced HTCL in tension-tension fatigue

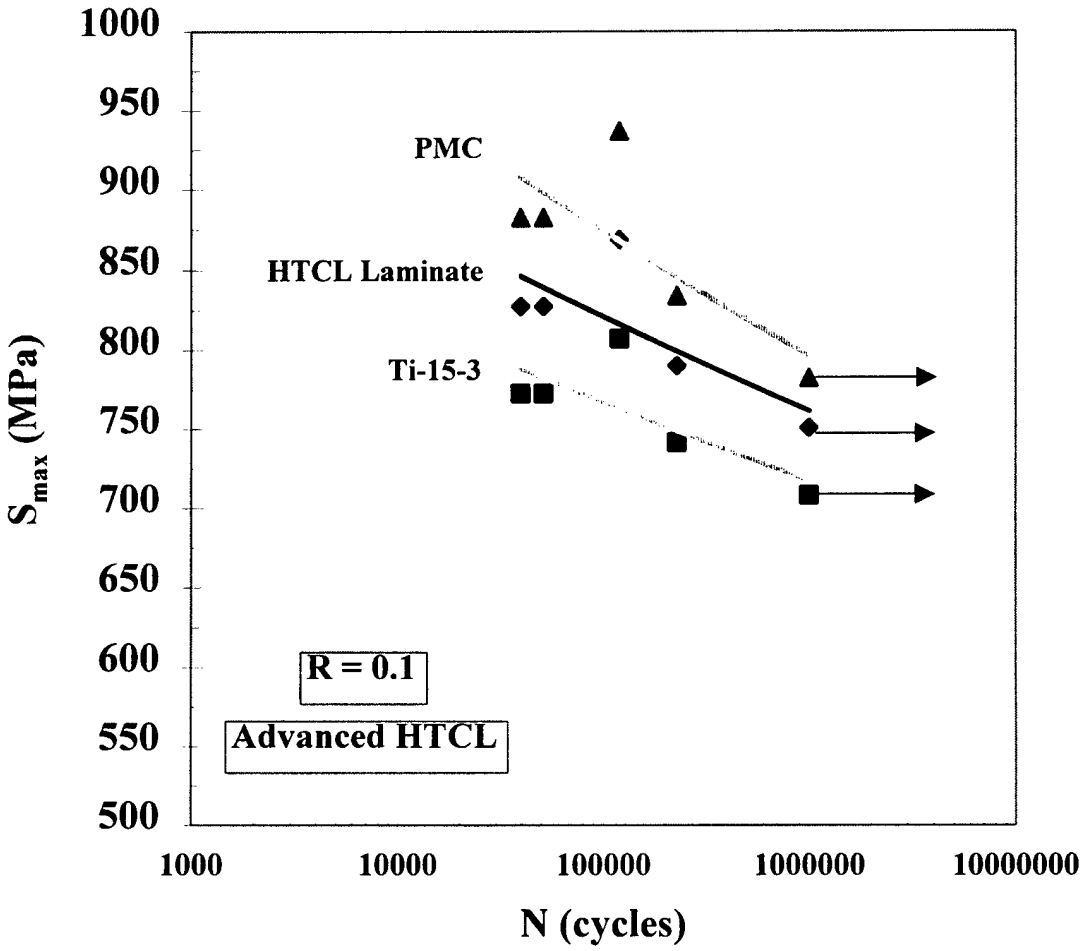

Figure 6.6 Load carrying capabilities of constituent plies of the HTCL laminate accounting for residual stresses.

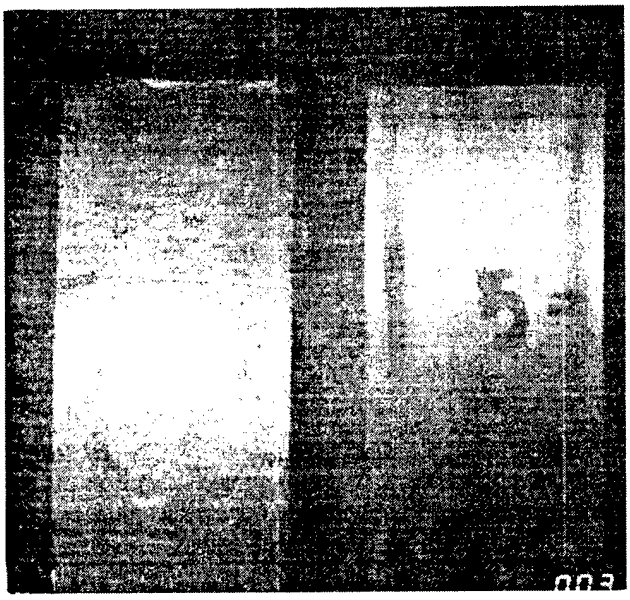

Figure 6.7 Comparison of advanced HTCL surfaces showing effects of rotary tool sanding (on left) and hand sanding.

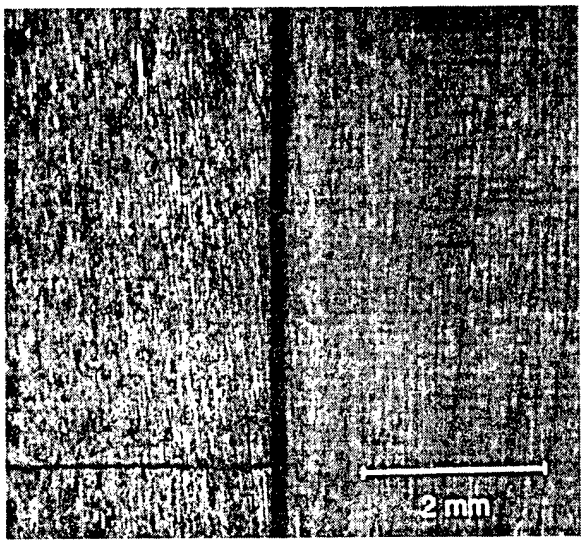

Figure 6.8 Close up of advanced HTCL surfaces (16 X magnification) with surface defects from rotary tool on left and hand sanded surface on right.

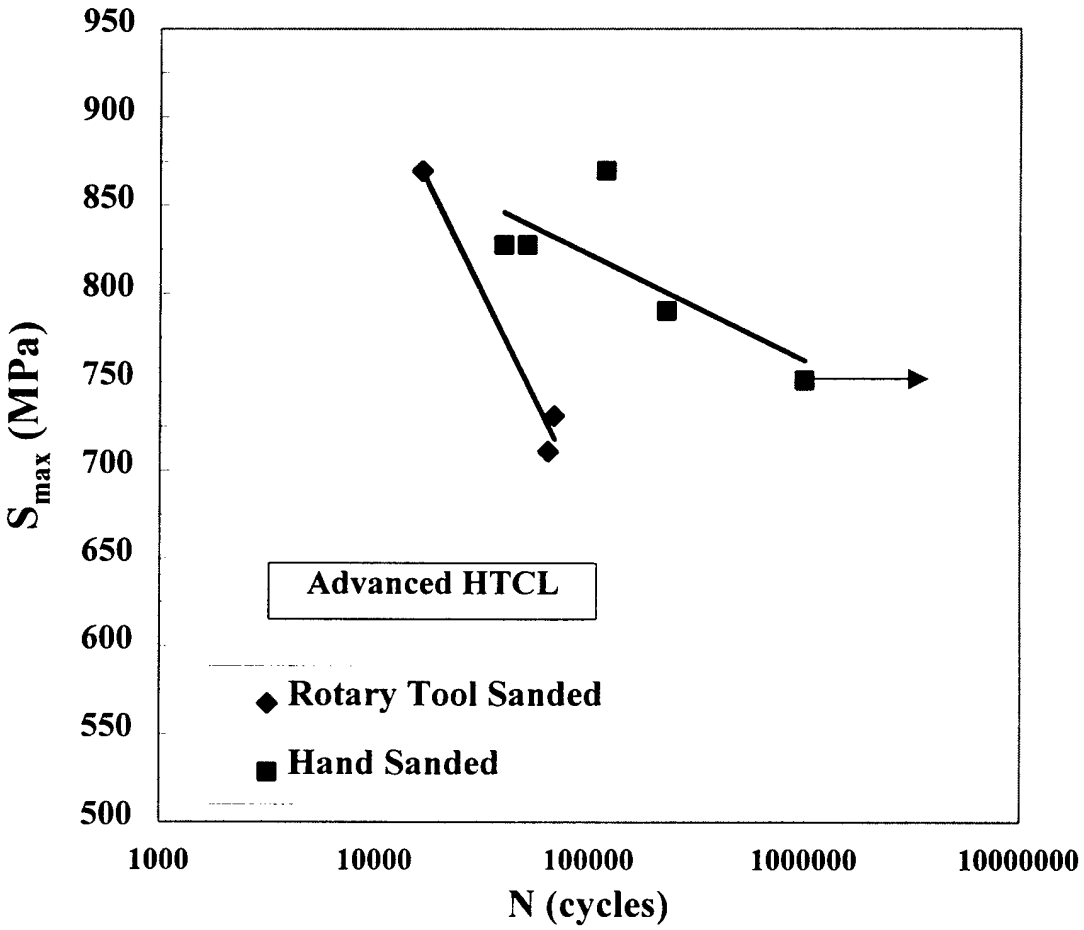

Figure 6.9 S-N curves for advanced HTCL showing effect of oxide removal sanding techniques

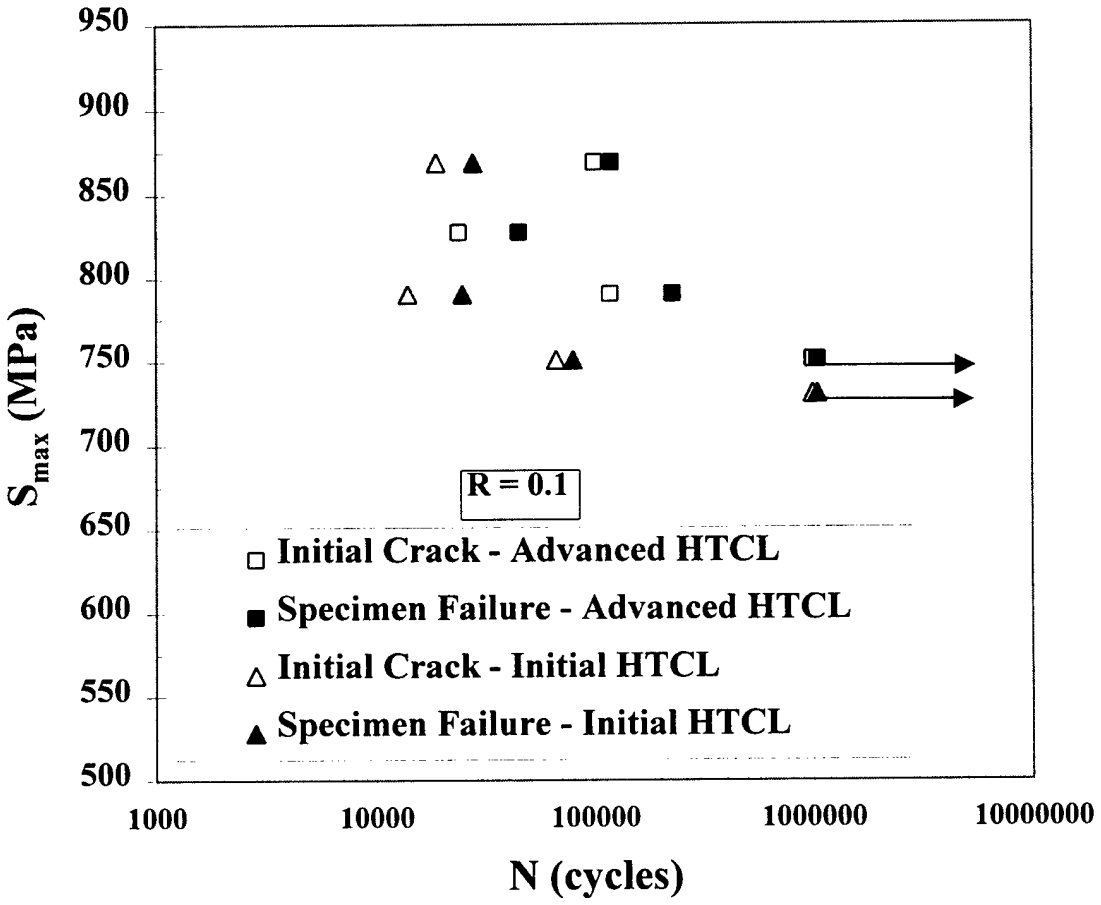

Figure 6.10 Comparison of first crack damage to specimen failure for initial and advanced HTCL in tension-tension loading

Figure 6.11 Close up of crack formed in titanium ply following 100,000 cycles of fatigue at S_{max}= 869 MPa, R = 0.1. (80 X magnification)

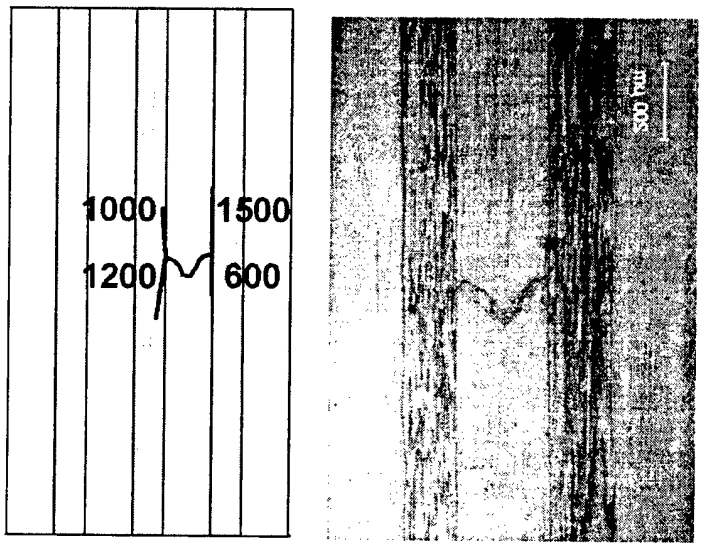

Figure 6.12 Replication and schematic of HTCL front edge showing fatigue crack and damage after 100,000 cycles. (S_{max} = 869 MPa, R = 0.1)

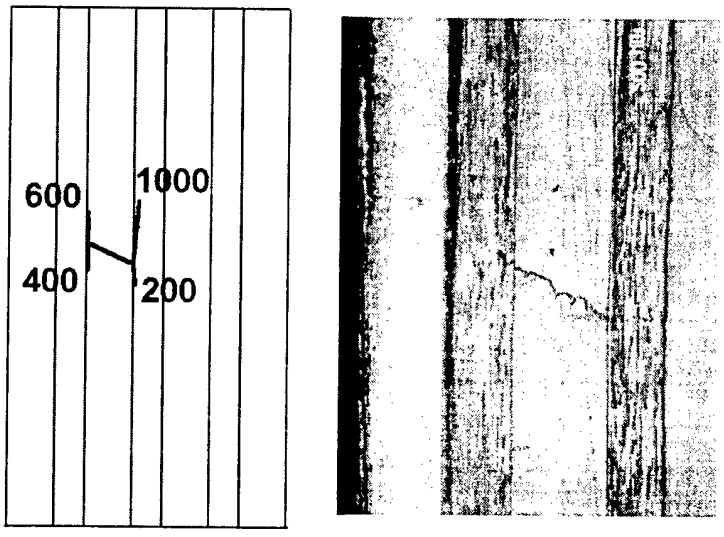

Figure 6.13 Replication and schematic of HTCL back edge showing fatigue crack and damage after 100,000 cycles. (S_{max} = 869 MPa, R = 0.1)

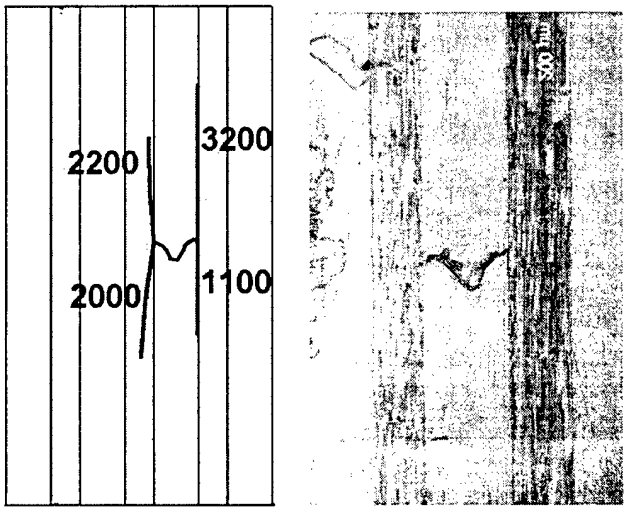

Figure 6.14 Replication and schematic of HTCL front edge showing fatigue crack and damage after 105,000 cycles. (S_{max} = 869 MPa, R = 0.1)

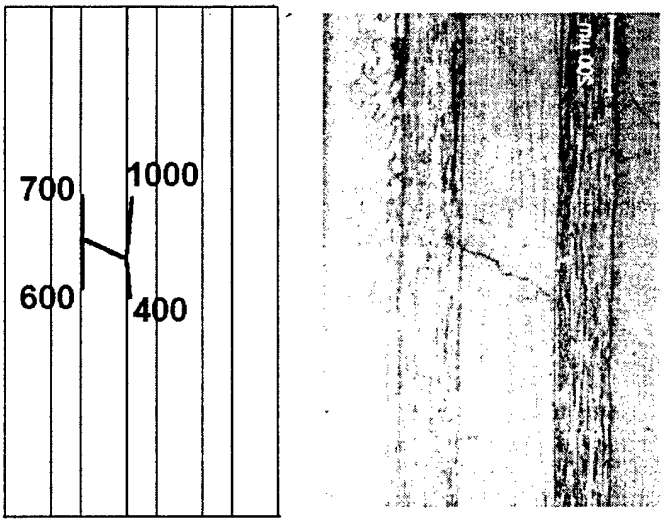

Figure 6.15 Replication and schematic of HTCL back edge showing fatigue crack and damage after 105,000 cycles. (S_{max} = 869 MPa, R = 0.1)

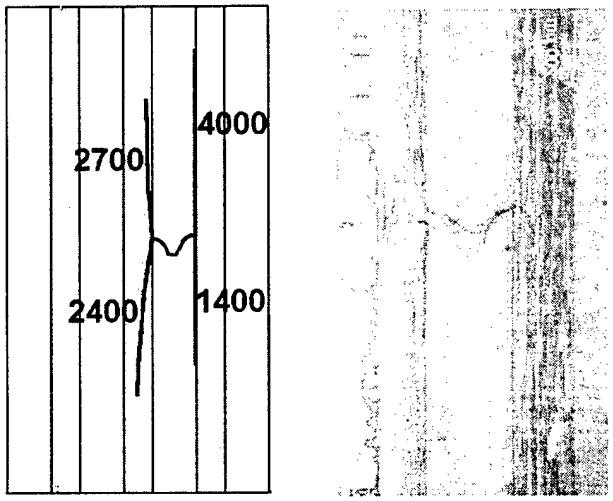

Figure 6.16 Replication and schematic of HTCL front edge showing fatigue crack and damage after 110,000 cycles. (S_{max} = 869 MPa, R = 0.1)

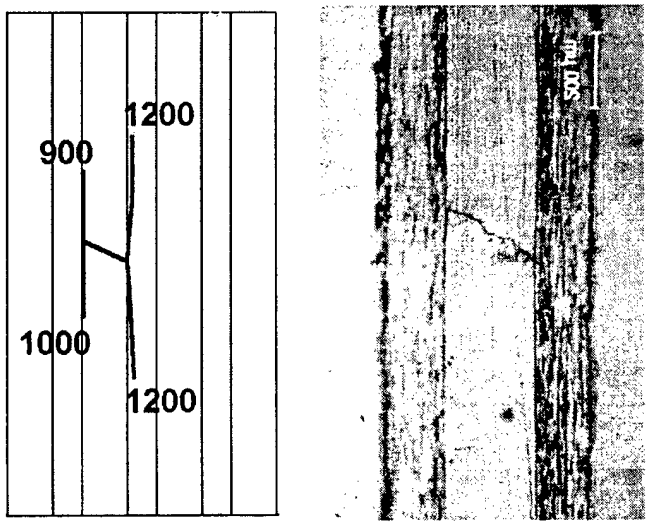

Figure 6.17 Replication and schematic of HTCL back edge showing fatigue crack and damage after 110,000 cycles. (S_{max} = 869 MPa, R = 0.1)

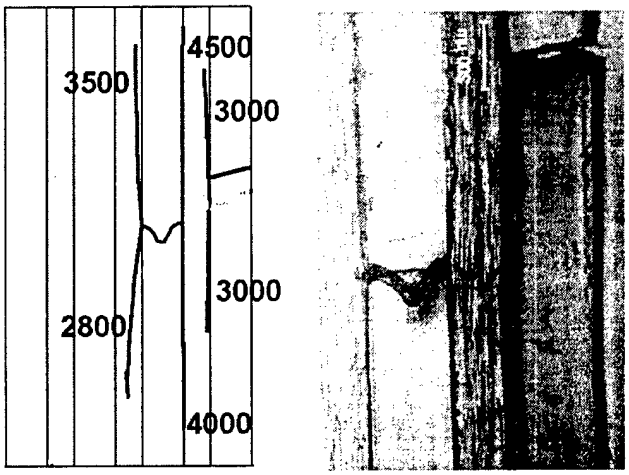

Figure 6.18 Replication and schematic of HTCL front edge showing fatigue crack and damage after 115,000 cycles showing adjacent titanium ply initiation. (S_{max} = 869 MPa, R = 0.1)

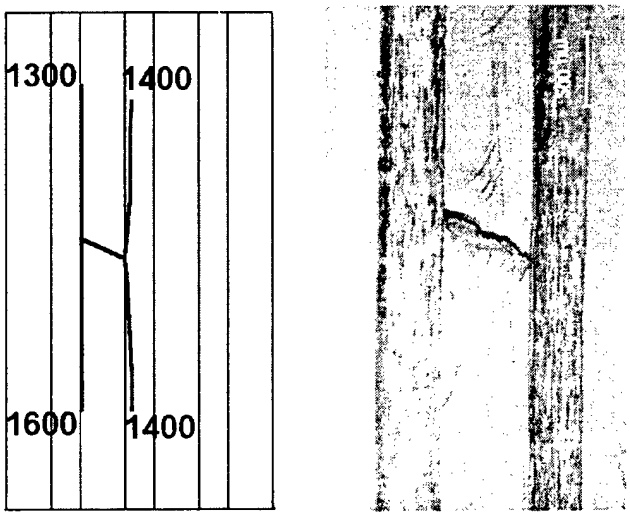

Figure 6.19 Replication and schematic of HTCL back edge showing fatigue crack and damage after 115,000 cycles. (S_{max} = 869 MPa, R = 0.1)

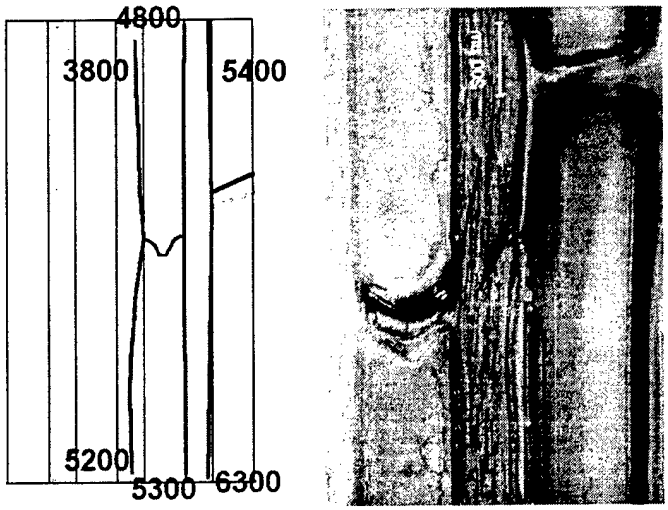

Figure 6.20 Replication and schematic of HTCL front edge showing fatigue crack and damage after 116,000 cycles. (S_{max} = 869 MPa, R = 0.1)

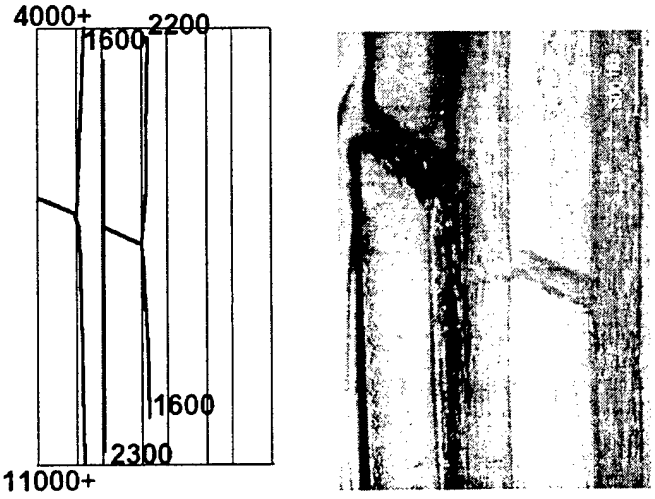

Figure 6.21 Replication and schematic of HTCL back edge showing fatigue crack and damage after 116,000 cycles showing adjacent titanium ply having completely failed. (S_{max} = 869 MPa, R = 0.1)

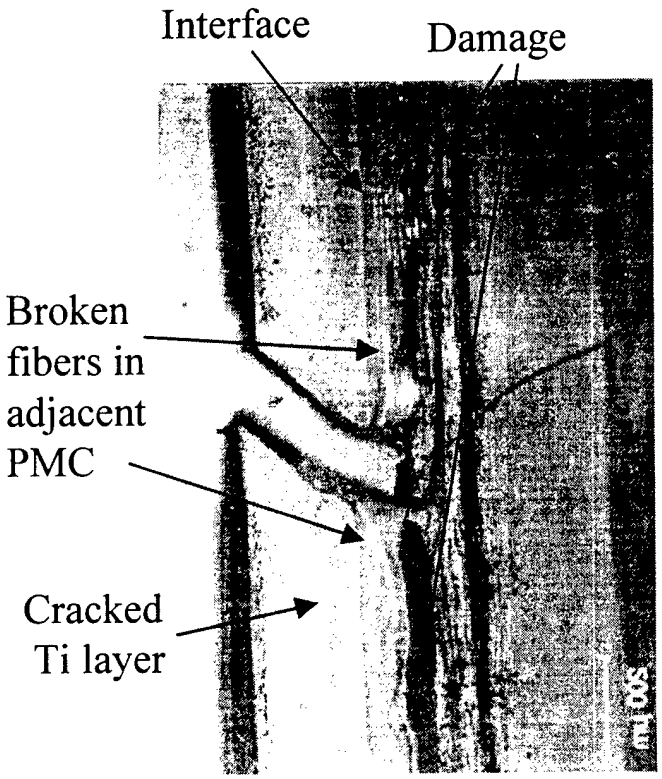

Figure 6.22 Replication of outer titanium ply having failed after 37,000 cycles (S_{max} = 827 MPa, R = 0.1). Note close to 50 % of PMC layer has remained bonded to titanium, preventing interfacial delamination.

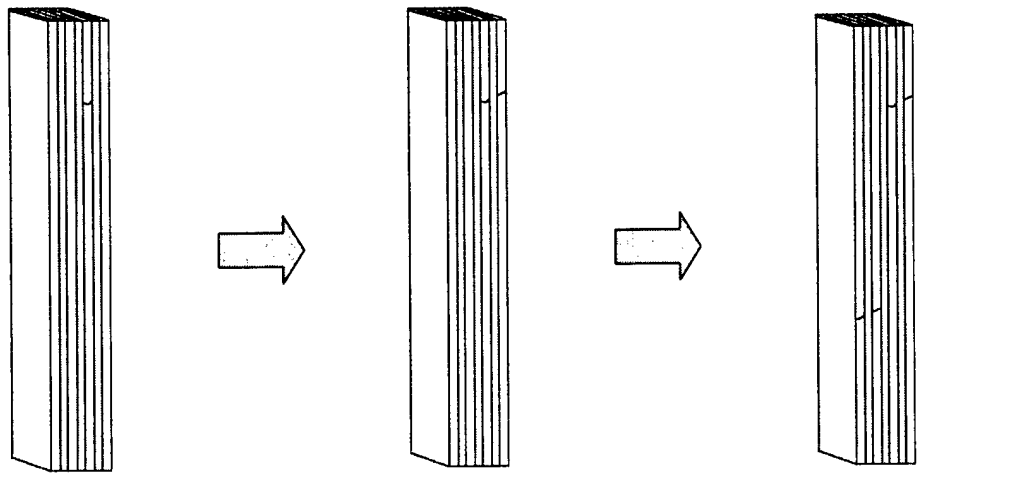

Figure 6.23 Titanium damage sequence showing number of cycles for each titanium ply cracking for S_{max} = 869 MPa, R = 0.1. The final two plies crack near simultaneously at specimen failure.

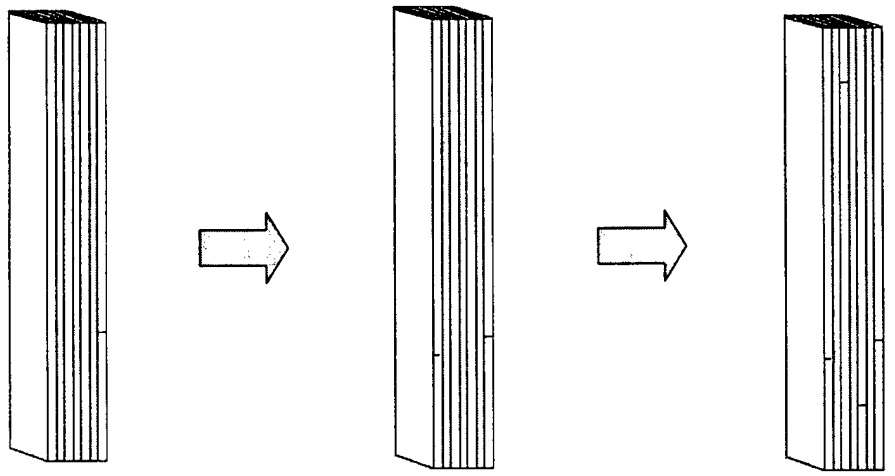

Figure 6.24 Titanium damage sequence showing number of cycles for each titanium ply cracking for S_{max} = 827 MPa, R = 0.1. The final two plies crack near simultaneously at specimen failure.

Figure 6.25 Lower portion of advanced HTCL titanium ply after failure showing fibers bonded to adjacent titanium. (Same inner ply shown cracked in Figure 6.12) Damage is characteristic of inner ply progression for tension-tension fatigue, with interfacial delamination progressing for limited distance before effectually delaminating between fibers.

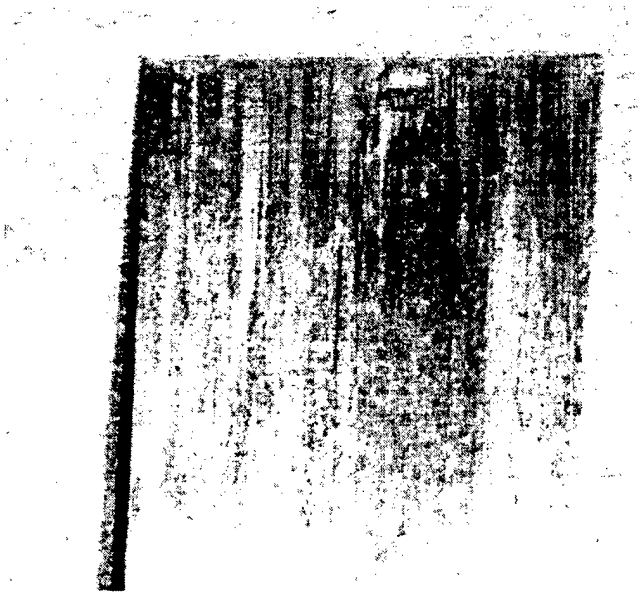

Figure 6.26 Lower portion of advanced HTCL outer titanium ply after failure. (Same outer ply shown cracked in Figure 6.18.) Damage is characteristic of outer ply progression for tension-tension fatigue, with fibers remaining bonded across entire ply.

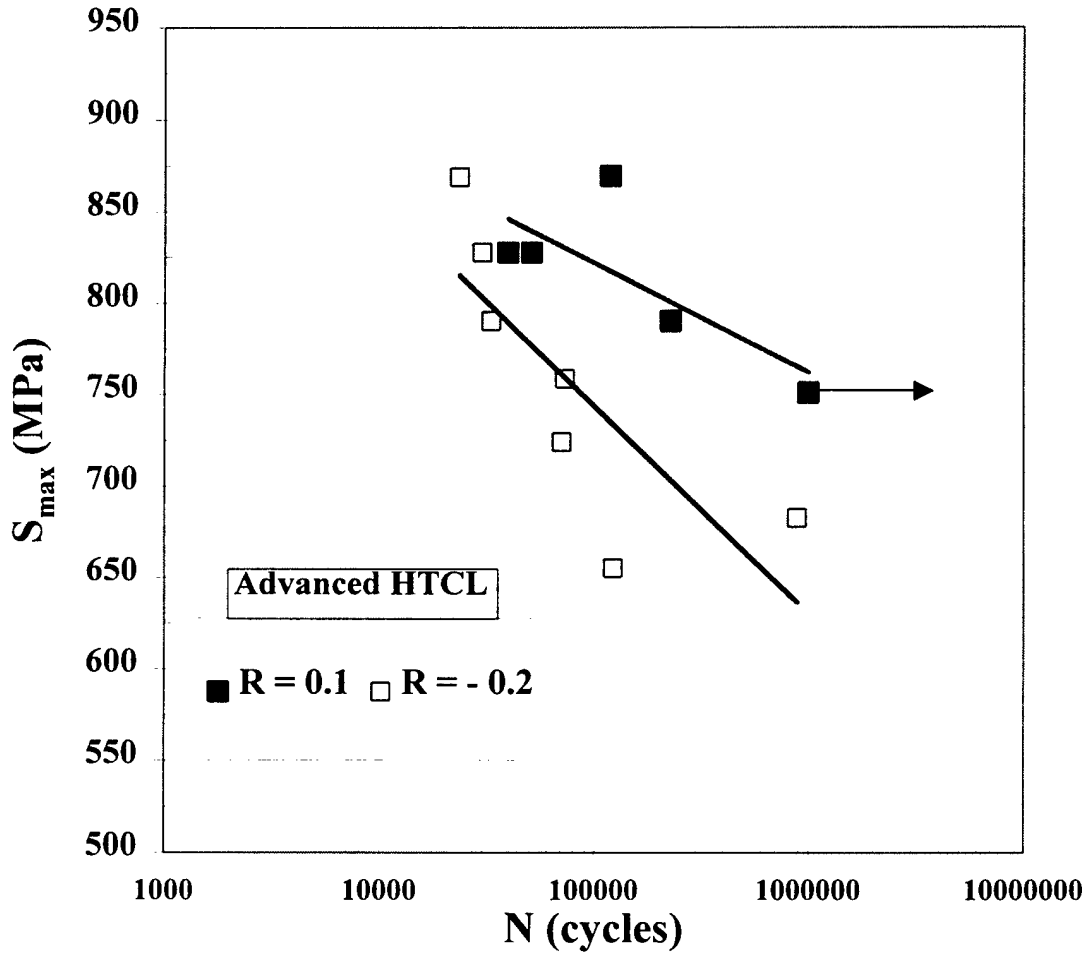

Figure 6.27 Experimental S-N data comparing advanced HTCL fatigue at R = 0.1 to R = -0.2.

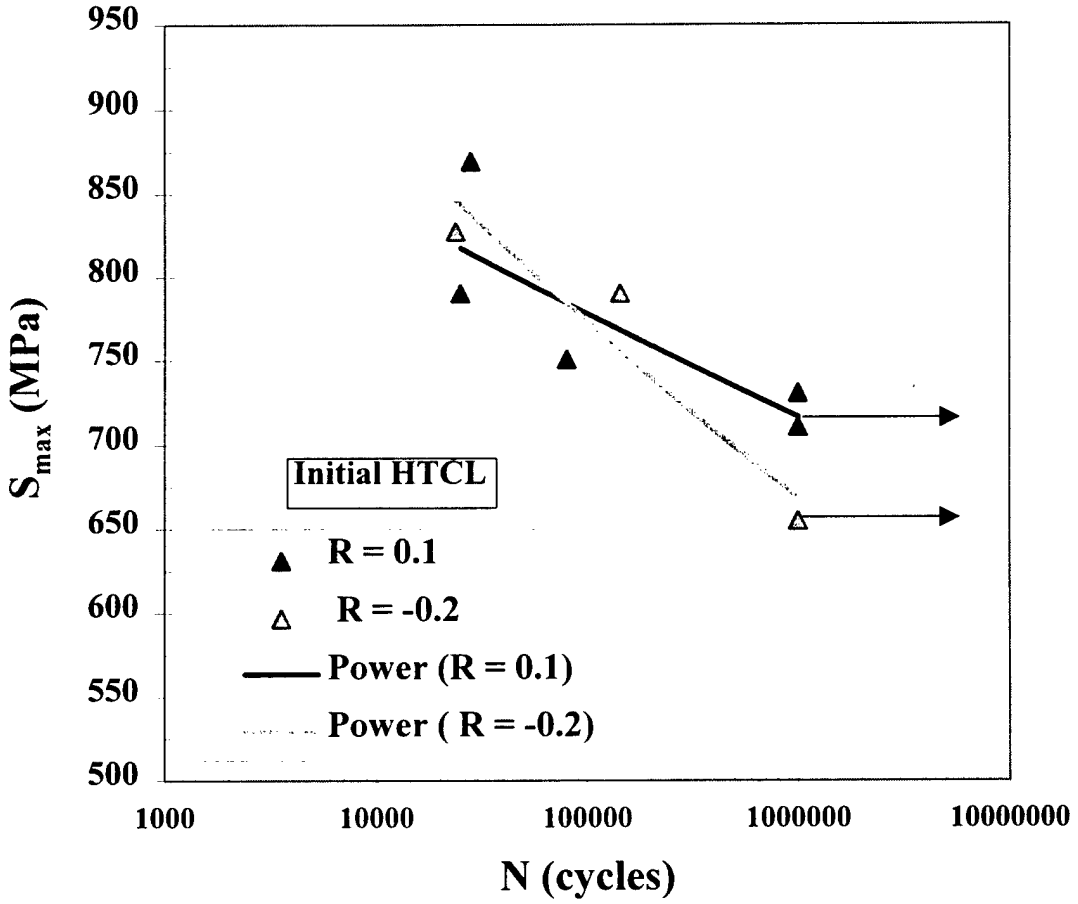

Figure 6.28 Experimental S-N data comparing initial HTCL fatigue at R = 0.1 to R = -0.2.

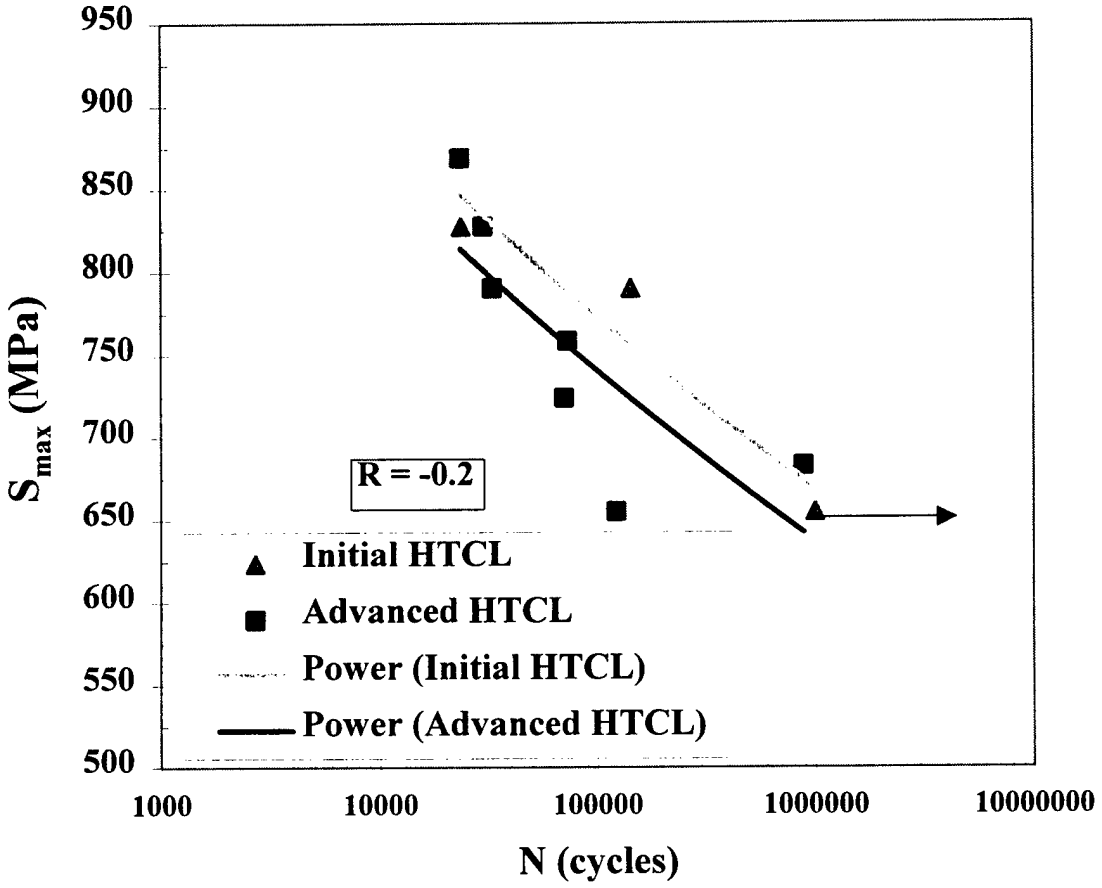

Figure 6.29 S-N curve comparison between fatigue of initial and advanced HTCL in tension-compression fatigue

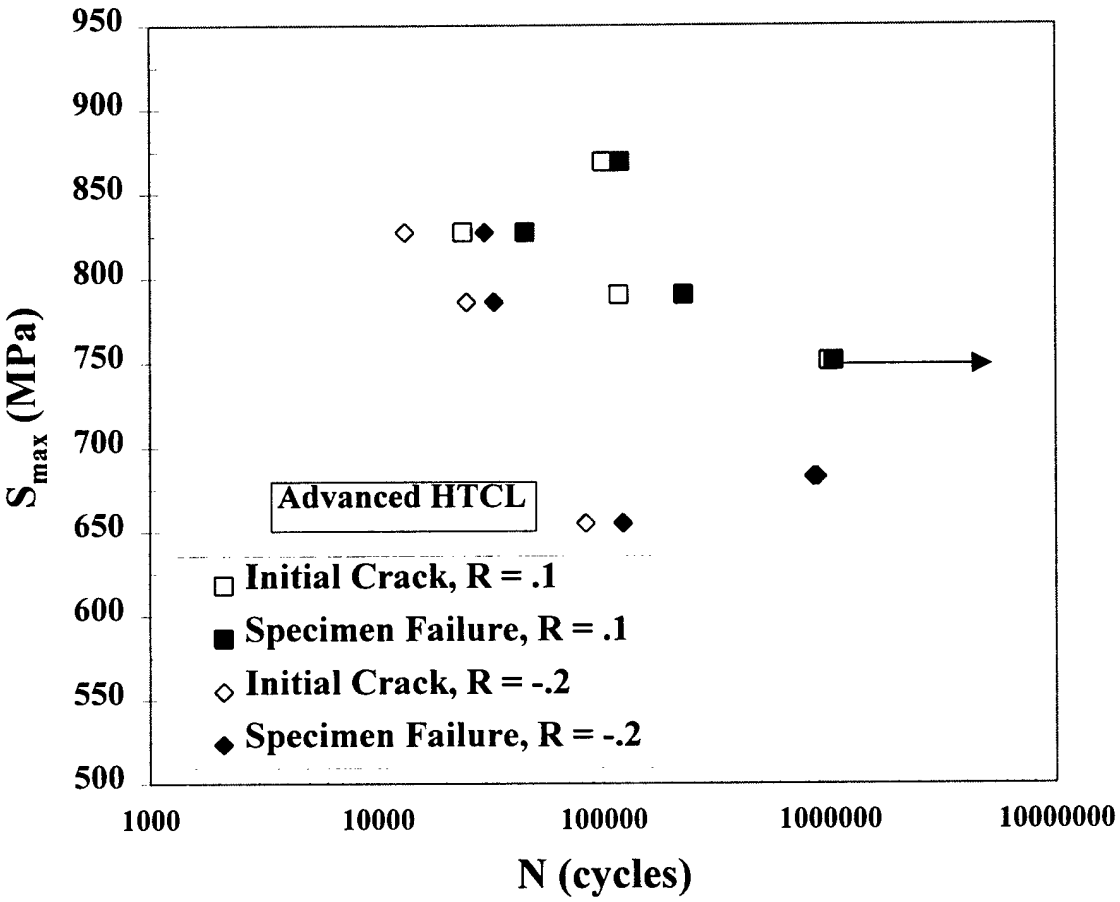

Figure 6.30 Comparison of initial titanium ply and specimen failure for advanced HTCL at R = 0.1 and R = -0.2.

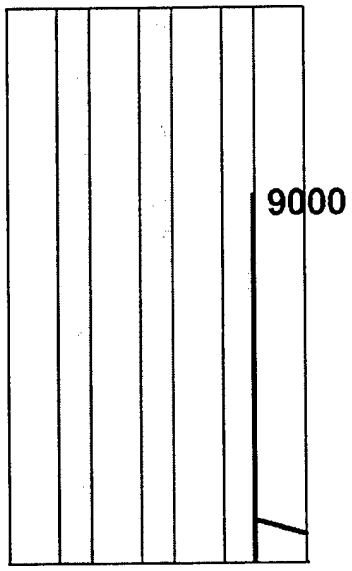

Figure 6.31 Advanced HTCL at 83,800 cycles (S_{max} = 655 MPa, R = -0.2) Crack initiates in outer ply and delamination begins at interface

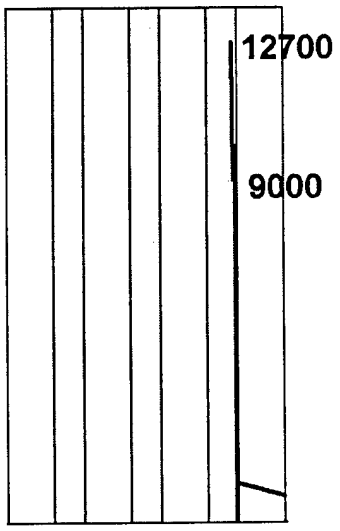

Figure 6.32 Advanced HTCL at 87,800 cycles (S_{max} = 655 MPa, R = -0.2) Initial crack delamination propagates to PMC layer

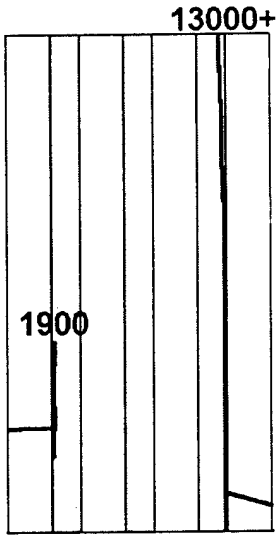

Figure 6.33 Advanced HTCL at 103,000 cycles (S_{max} = 655 MPa, R = -0.2) Initial crack damage beyond replication, second titanium ply fails/propagates damage

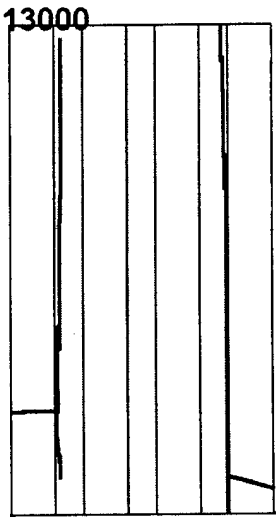

Figure 6.34 Advanced HTCL at 113,000 cycles, (S_{max} = 655 MPa, R = -0.2) Second crack damage propagates into PMC layer

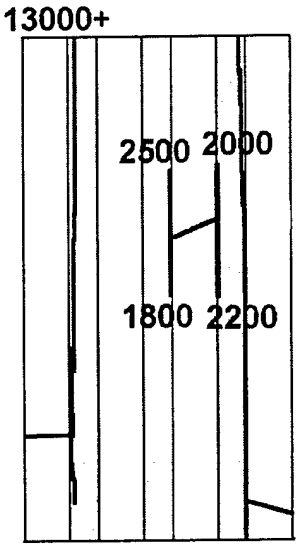

Figure 6.35 Advanced HTCL at 113,700 cycles, (S_{max} = 655 MPa, R = -0.2) Third crack initiates at inner ply.

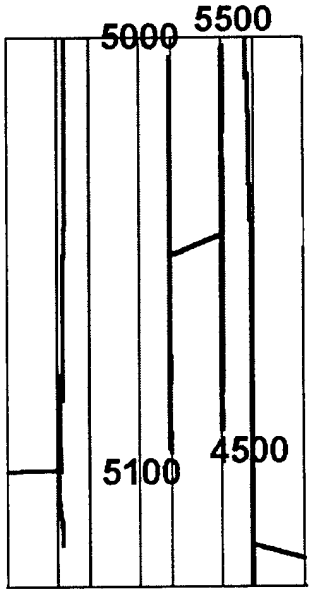

Figure 6.36 Advanced HTCL at 117,000 cycles, (S_{max} = 655 MPa, R = -0.2) Third crack damage propagates along interface.

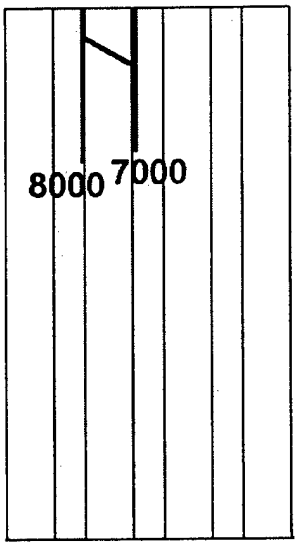

Figure 6.37 Initial HTCL at 141,600 cycles (S_{max} = 786 MPa, R = -0.2) Crack initiates in inner ply and delamination begins.

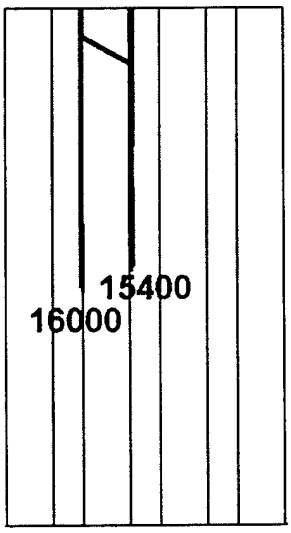

Figure 6.38 Initial HTCL at 142,700 cycles (S_{max} = 786 MPa, R = -0.2) Delamination continues.

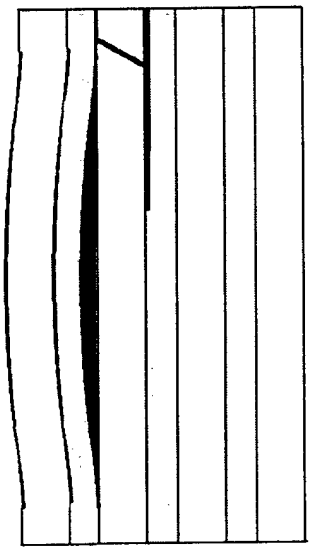

Figure 6.39 Initial HTCL at 143,250 cycles (S_{max} = 786 MPa, R = -0.2) Delamination propagates along entire specimen and ply begins buckling

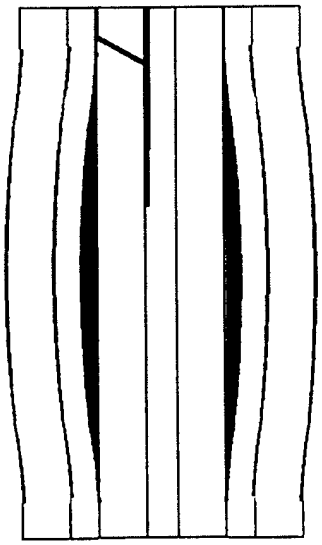

Figure 6.40 Initial HTCL at 143,340 cycles (S_{max} = 786 MPa, R = -0.2) Opposite outer ply begins buckling

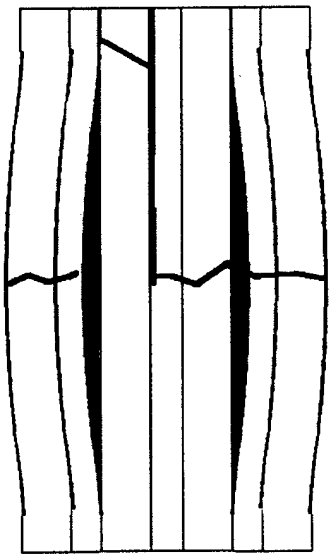

Figure 6.41 Initial HTCL at 143,371 cycles (S_{max} = 786 MPa, R = -0.2) Specimen failure

Figure 6.42 Advanced HTCL inner ply surface following tension-compression fatigue. Note fibers bonded to titanium ply.

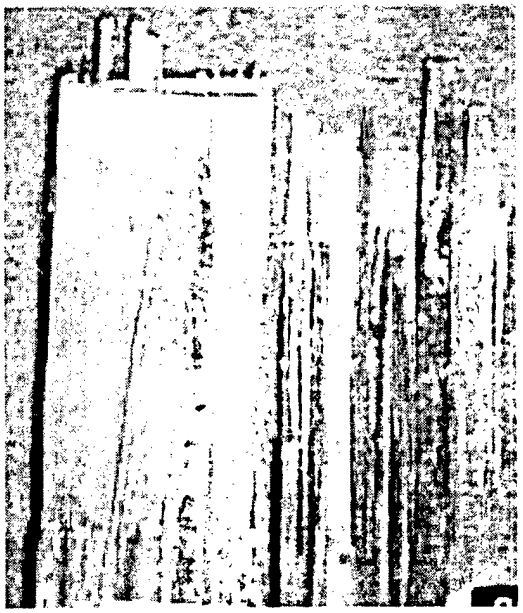

Figure 6.43 Initial HTCL inner ply surface following tension-compression fatigue. Note, mostly bare titanium ply with no fibers remaining bonded.

CHAPTER VII

CONCLUSIONS

The goal of this research was to determine how HTCL performed in fatigue after incorporating the PMC matrix/titanium surface treatment combination which was most effective at limiting delamination at the Ti/PMC interface. The advanced HTCL proved more resistant to this condition in both tension-tension and tension-compression in comparison to the initial HTCL construction because of this strengthened interface. The advanced laminate showed a greater damage tolerance, specifically evident in the cycles-to-failure following initial titanium ply damage. Such improvement is a significant advantage in aerospace applications in that reasonable inspection intervals following damage initiation can be developed for a component designed from advanced HTCL. Furthermore, the amount of PMC fibers remaining bonded to failed titanium, in either tension-tension or tension-compression, demonstrated the advanced laminates resistance to separation along the ply interface. However, the overall fatigue life of the advanced HTCL did not show significant improvement over the initial HTCL as a result of this improvement.

The reason this obviously strengthened interface did not produce a substantially longer lasting material is mostly a function of when the titanium damage begins, but there is some indication that interface may be slightly too strong. Even though the titanium

damage to failure life was extended under compressive loading due to this strength, in both loading conditions, fibers adjacent to this titanium damage were broken. This must result in a loss of PMC strength, which have already been proven to carry the bulk of tensile as well as fatigue loads [1]. Though titanium ply damage did not significantly propagate through the entire specimen thickness or along the interface, the adjacent PMC layer suffered from enough Mode I tearing and mixed mode peeling to prevent any substantial increase in HTCL fatigue life. Furthermore, the damage tolerance inherent to hybrid composite laminates relies on fiber-bridging. Any failure of PMC layers only reduces the capabilities of this mechanism.

However, since the overall life did not decrease, the interface was not strengthened to castrostrophic levels just as dangerous as a fragile interface. As Marissen [18] argues, possessing an infinitely strong interface and thus preventing any delamination or adhesive shear deformation results in a metal crack unable to alleviate the stress concentration, limiting the damage tolerance of the laminate. Had an initial fatigue induced titanium crack rapidly produced specimen failure and/or resulted in cracking through the entire cross-section from that initial crack, the HTCL would possess far too strong of an interface. Neither occurred in the fatigue of advanced HTCL. Though titanium plies separated from the laminate taking some fibers with it, the stress concentration is still removed from the immediate area of damage initiation. Even though the interfacial bond remains strong, particularly in the Mode I/Mode II condition, the matrix bond between the fibers is weak enough in the presence of mixed mode loading to allow damage to propagate longitudinally away from the initiated crack. If

this resin matrix bond between the fibers is also strengthened, the stress concentration is not relieved and the crack may propagate completely through the material.

The advanced HTCL possesses a significantly stronger interface than the initial HTCL resulting in a more damage tolerant laminate, however a more optimized combination of adhesive resin and titanium surface treatment combination may still exist. The history of hybrid composite materials has proven that a fine balance in interfacial strength must be maintained with neither extremely high nor low strength being favorable. A laminate with the optimal interfacial strength permits stable, controlled delamination, preferably at the interface. Nevertheless HTCL has certainly been improved and definitely "advanced" over the initial construction.

CHAPTER VIII

RECOMMENDATIONS

HTCL was designed as a strong, damage tolerant aerospace material capable of superior fatigue performance at elevated temperatures. However such capabilities, especially following damage, are contingent upon the load interactions of the constituents, which prove a very delicate balance. As was concluded, the strengthening of advanced HTCL has likely pushed the interfacial improvement too far. The failure of PMC fibers is certainly not a favorable damage mechanism for hybrid composite fatigue, therefore further investigation for a slightly weaker interface is warranted.

If such testing is accomplished, both end notch flexure (ENF) as well as cracked lap shear (CLS) tests should, perhaps, be investigated. Recall that in the initial testing of adhesive resin/Ti surface treatment combinations by Cobb, [2] CLS specimens were used as history indicated that outer titanium ply cracking was the assumed initial damage state. Since the CLS specimens adequately model the mixed mode behavior created by an outer ply failure, such testing is certainly validated. However, the current research has determined the initial titanium ply failure can occur at an inner ply. No matter when it occurs, inner titanium ply failure creates mostly Mode II type behavior, which is best tested using ENF specimens.

However, the HTCL of the current construction has yet to be tested at the elevated temperature (350°F) for which it was designed. Though significant improvement in fatigue performance due to the interface is not likely, it is possible. Benefits at elevated temperature of HTCL have already been observed due to the relieving of residual stresses in the titanium induced in processing. However, improvement of the advanced HTCL must come from a weakened interface. Such might result due to an environmental effect.

APPENDIX

TEST SET-UPS/EQUIPMENT

This appendix reveals the test frames and equipment used in the current research as discussed in Chapter 4. All equipment is located in the Materials Properties Research Laboratory in the Bunger-Henry Building.

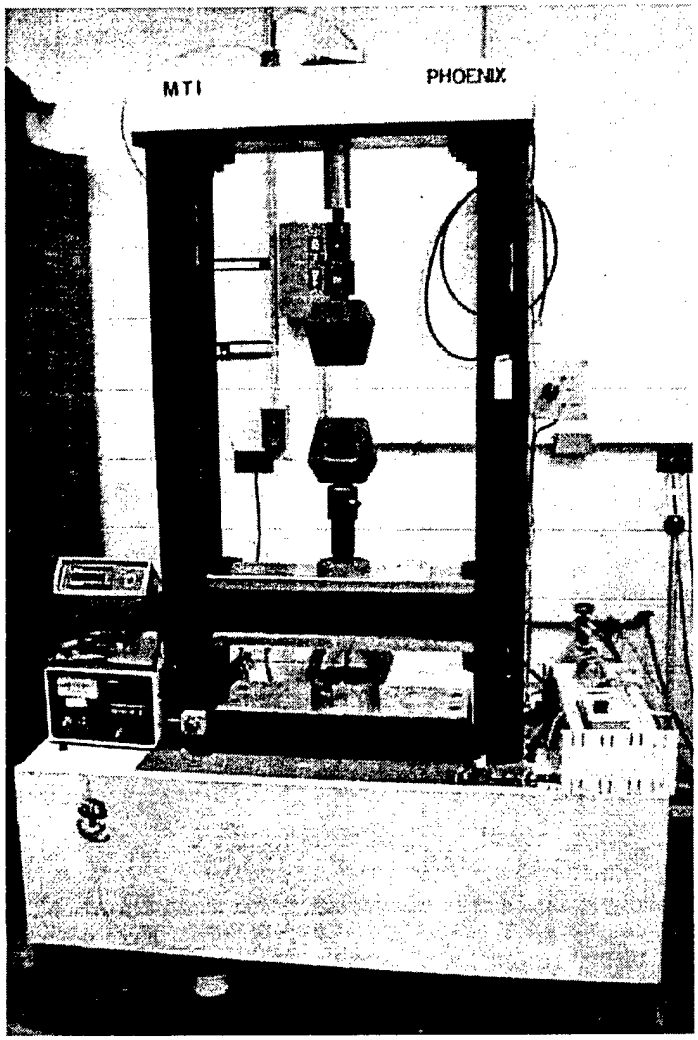

Figure A.1 Screw-driven test frame with 10 metric ton (22 kip) load cell

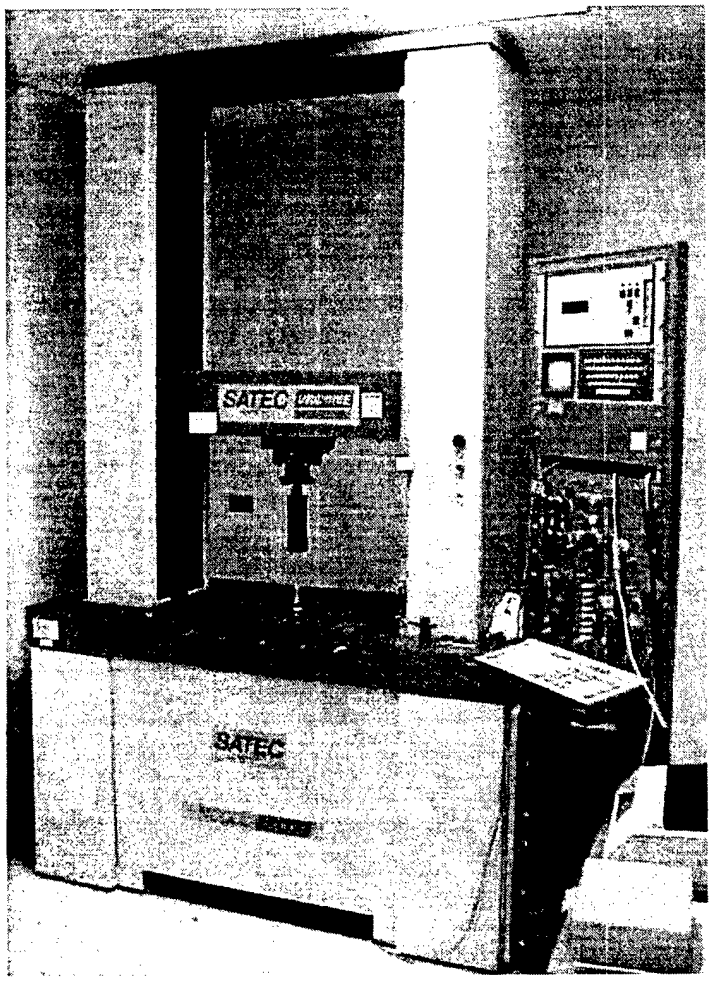

Figure A.2 Screw-driven test frame with 25 metric ton (50 kip) load cell

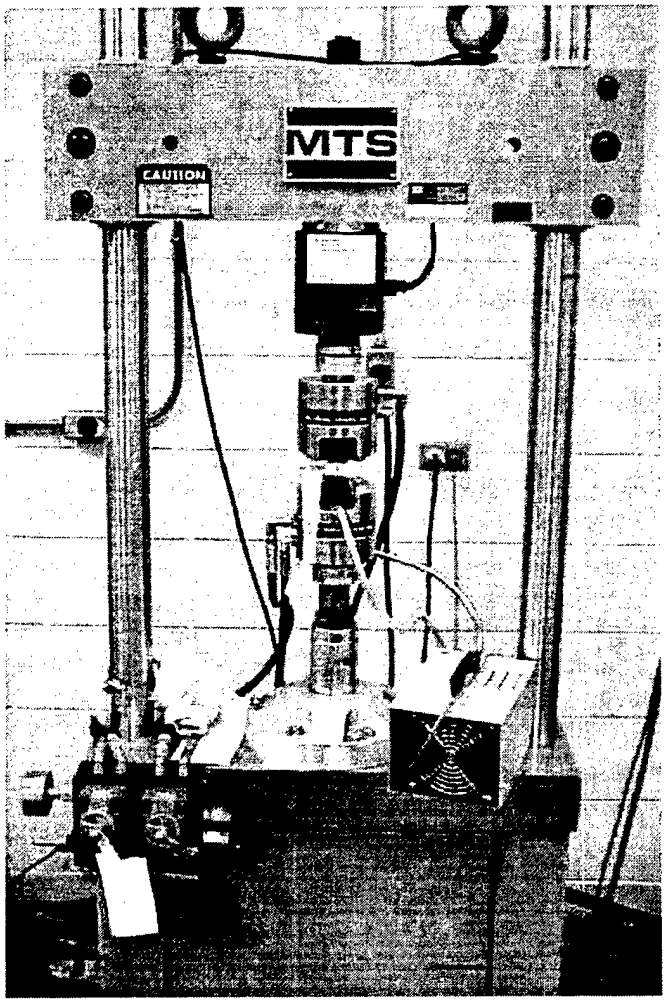

Figure A.3 Servo-hydraulic test frame with 25 kN (5.5 kip) load cell

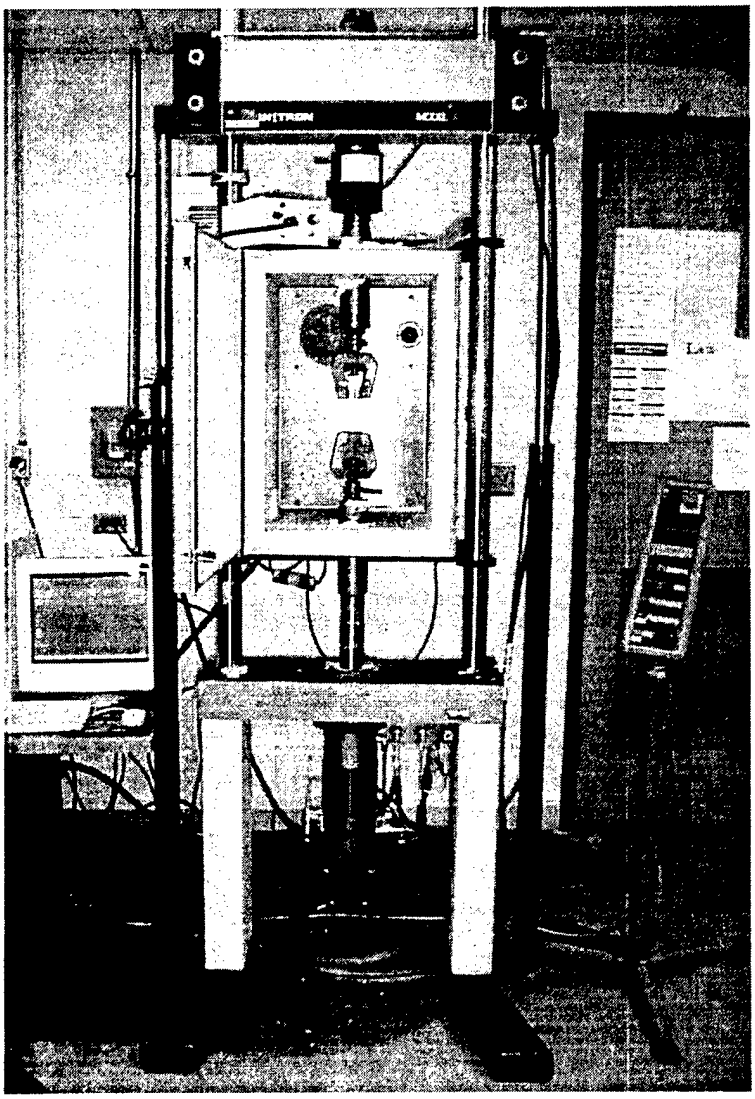

Figure A.4 Servo-hydraulic test frame with 10 metric ton (22 kip) load cell

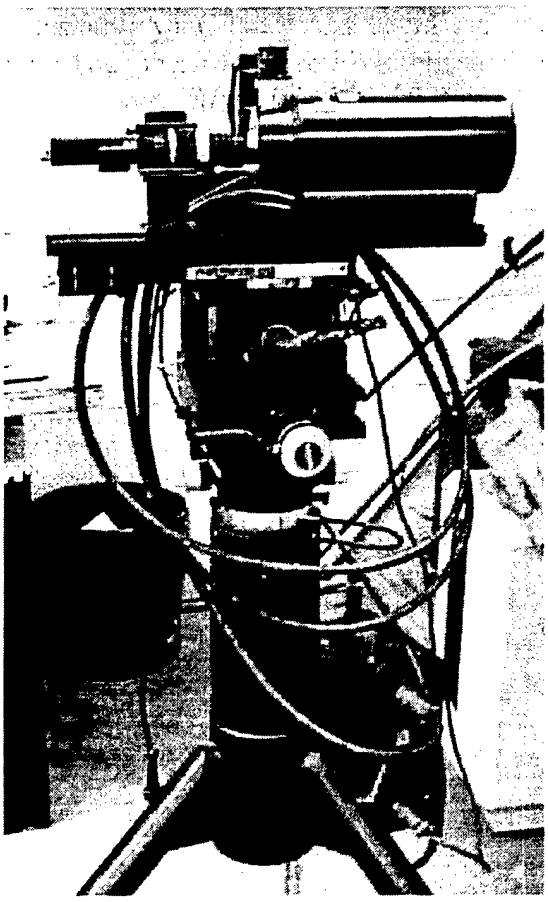

Figure A.5 Traveling telemicroscope

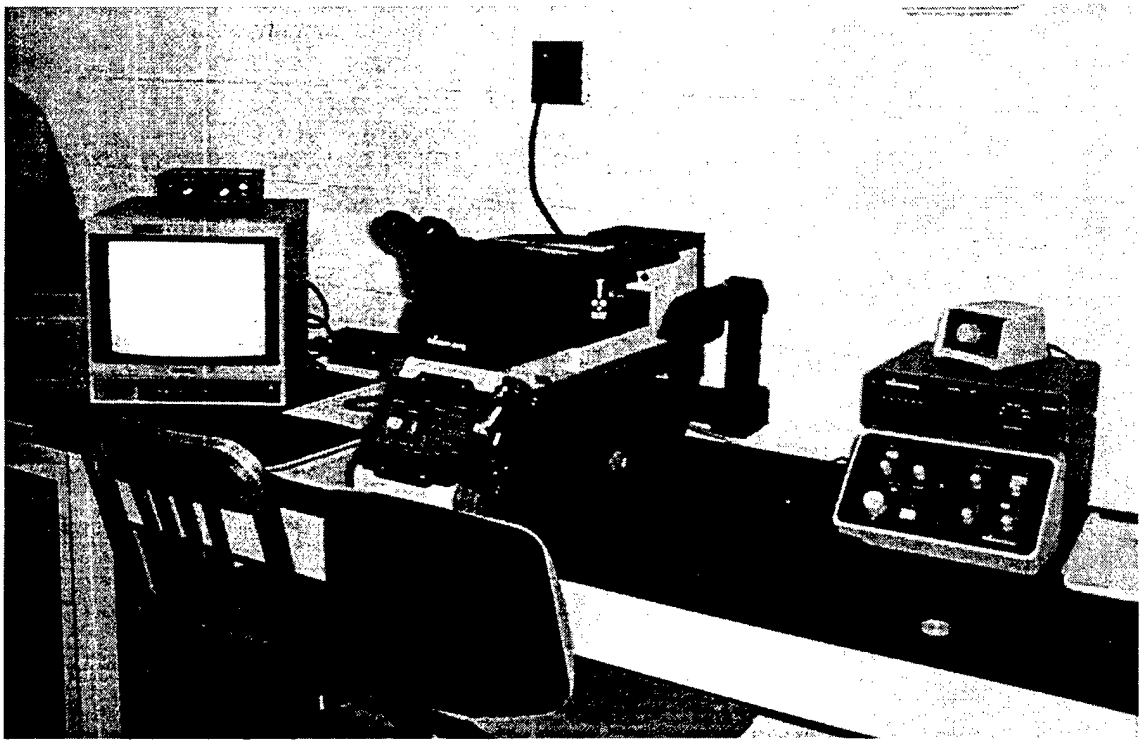

Figure A.6 Optical microscope with instant camera

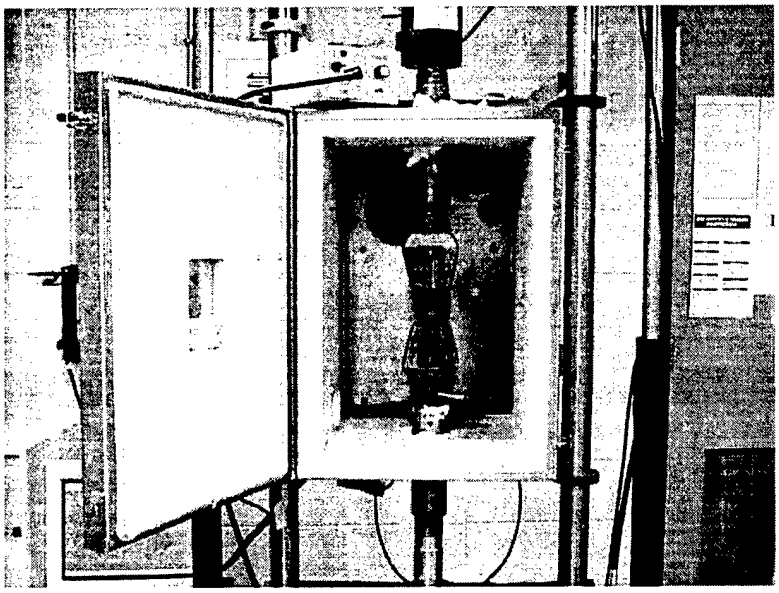

Figure A.7 Environmental chamber showed mounted on a test frame

REFERENCES

[1] Li, E, Johnson, W.S., An Investigation into the Fatigue of Hybrid Titanium Composite Laminate, *Journal of Composites Technology & Research*, JCTRER, Vol. 20, No. 1, January, 1998, pp. 3-12.

[2] Cobb, T., Johnson, W.S., Lowther, S.E., St. Clair, T.L., Optimization of Surface Treatment and Adhesion Selection for Bond Durability in Ti-15-3 Laminates, Journal of Adhesion, Vol. 71, 1999, pp. 115-141.

[3] Mallick, P.K., Fiber-Reinforced Composites, Second Edition, Marcel Dekker, Inc. c. 1993

[4] Krishnakumar, S. "Fiber Metal Laminates" – The Synthesis of Metals and Composites," *Materials and Manufacturing Processes*, Vol. 9, No. 2, 1994, pp. 295-354

[5] Lawcock, G.D., Ye, L., Mai, Y., Sun, C., "Effects of Fibre/Matrix Adhesion on Carbon-Fibre-Reinforced Metal Laminates-Impact Behavior," *Composite Science and Technology*, Vol. 57, No. 12, Dec 1997, pp. 1609-1619

[6] Asundi, A., Choi, A., "Fiber Metal Laminates: An Advanced Material for Future Aircraft," *Journal of Materials Processing Technology*, Vol. 63, Jan 1997, pp. 384-394

[7] Johnson, W.S., Morrow, J.W., Little, C.D., "Damage Tolerance Crack Growth Characterization of 7475 Aluminum Material," Research Report, Research & Engineering Departments, General Dynamics Corp., Dec 1976

[8] Kaufman, J.G., "Fracture Toughness of 7075-T6 and –T651 Sheet, Plate and Multilayered Adhesive-Bonded Panels," *Journal of Basic Engineering*, Vol. 89, 1967, pp. 503-507.

[9] Johnson, W.S., Rister, W.C. and Spamer, T., "Spectrum Crack Growth in Adhesively Bonded Structure," *Journal of Engineering Materials and Technology*, ASME, Vol. 100, 1978, pp. 57-63.

[10] Johnson, W.S., "Damage Tolerance Evaluation of Adhesively Laminated Titanium," *Journal of Engineering Materials and Technology*, ASME, Vol. 105, 1983, pp. 182-187.

[11] Verbruggen, M., "Aramid Reinforced Aluminum Laminates: ARALL," Report LR-503, Delft University of Technology, November 1986

[12] Young, J.B., Landry, J.G.N., Cavoulacos, V.N., "Crack Growth and Residual Strength Characteristics of Two Grades of Glass-reinforced Aluminum 'Glare'," *Composite Structures* Vol. 27, 1994, pp. 457-469.

[13] Grabilnikov, A.S., Mashinskaya, G.P. Zhelezina, G.F., Zinevich, O.M., Deyev, I.S., "Interlaminar Fracture Toughness of a Hybrid Composite Material of the ALOR Type," *Mechanics of Composite Materials*, Vol. 30, No. 2, 1994, pp. 136-145

[14] Freischmidt, G., Coutts, R.S.P., Janardhana, M.N., "Aluminum/lithium Alloy-Carbon Fibre/Epoxy Laminated Hybrid Composite Material Part I, Preliminary Results," *Journal of Materials Science Letter*, Vol. 13, 1994, pp. 1027-1031

[15] Miller, J.L., Progar, D.J., Johnson, W.S., St.Clair, T.L., "Preliminary Evaluation of Hybrid Titanium Composite Laminates," NASA Technical Memorandum 109095, National Aeronautics and Space Administration, Langley Research Center, Hampton, Virginia 23681-0001, April 1994.

[16] Pagano, N.J. Interlaminar Response of Composite Materials, Composite Materials Series, Vol. 5, Elsevier Science Publishing Co., c.1989.

[17] Armanios, E, Rehfield, L., Weinstein, F., Reddy, A., "Interlaminar Fracture of Composites Under Tension and Compression," Journal of Aerospace Engineering, Vol. 3, No. 1, January, 1990, pp. 30-45.

[18] Marissen, R. "Fatigue Crack Growth in ARALL-A Hybrid Aluminum-Aramid Composite Material," Report LR-574, Delft University of Technology, June 1988

[19] Ritchie, R.O., Yu, Weikang, Bucci, R.J., "Fatigue Crack Propagation in ARALL Laminates: Measuring the Effect of Crack Tip Shielding From Crack Bridging," *Engineering Fracture Mechanics*, Vol. 32, No. 3, 1989, pp. 361-377

[20] Davidson, D.L., Austin, L.K., "Fatigue Crack Growth Through ARALL-4 @ Ambient Temperature," *Fatigue Fracture and Engineering Materials Structures*, Vol. 14, No. 10, 1991, pp. 939-951

[21] Macharet, J., Teply, J.L., Winter, E.F.M., "Delamination Shape Effects in Aramid-Epoxy-Aluminum (ARALL) Laminates with Fatigue Cracks," *Polymer Composites*, Vol. 10, No.5, Oct 1989, pp. 322-327

[22] Burianek, D., Spearing, S.M., "Fatigue Induced Delamination in Titanium-Graphite Hybrid Laminates." *Proceedings of the 13th Annual Technical Conference on Composite Materials*. September, 1998.

[23] Boyer, R., Welsch, G., Collings, E.W., Titanium Alloys, *ASM International*, pp. 899-919.

[24] Rosenberg, H.W., "Ti-15-3: A New Cold-Formable Sheet Titanium Alloy," *Journal of Metals*, November 1983, pp. 30-34.

[25] Smith Jr., J.G., Connell, J.W., Hergenrother, P.M., "The Effect of Phenylethynyl Terminated Imide Oligomer Molecular Weight on the Properties of Composites." Materials Division, NASA-Langley Research Center, 1999.

[26] St.Clair, T.L., NASA-Langley Research Center, 1999. Personal Communication.

[27] Li, E., Johnson, W.S., Lowther, S.E., and St. Clair, T.L., "An Evaluation of Two Fabrication Methods for Hybrid Titanium Composite Laminates," *Composite Materials: Testing and Design, Thirteenth Volume, ASTM STP 1242*, American Society for Testing and Materials, 1997, pp. 202-214.

[28] Li, E, An Investigation of Constant Amplitude Fatigue for Hybrid Titanium Composite Laminates at Elevated Temperatures, M.S. Thesis, Georgia Institute of Technology, Atlanta, GA, January, 1997.

[29] Theriault, R.P., Osswald, T.A., "Residual Stress Development During Laminate Processing," ANTEC, 1998, pp.758-762.

[30] Hergenrother, P.M., NASA-Langley Research Center, 1999. Personal Communication.

[31] Bahei-El-Din, Y.A., Dvorak, G.J. "Plasticity Analysis of Laminated Composite Plates," Journal of Applied Mechanics, Vol. 49, 1982, pp. 740-746.

[32] Li, E, Johnson, W.S., Miller, J., "High Temperature Hybrid Composite Laminates: An Early Analytical Assessment," proceedings for the Tenth International Conference on Composite Materials, ICCM-10, 1995.

[33] Wu, H.F., Wu, L.L., Slagter, W.J., Verolme, J.L., "Use of Rule of Mixtures and Metal Volume Fraction for Mechanical Property Predictions of Fibre-reinforced Aluminum Laminates." Journal of Material Science, Vol 29, 1994, pp. 4583-4591.

VITA

Donald William Rhymer was born on March 2, 1973 to Peter (USAF Major, ret.) and Sue. Born as an Air Force brat with his sister Sue Anne, Donald learned the value of God and country, the importance and value of a good upbringing, and motivation to always strive for the best, particularly in education and learning. Shortly following his father's retirement, Donald set a goal to attend the U.S. Air Force Academy. A month following graduation from Parkersburg High School in 1991, he achieved that goal. As a Cadet, Donald became a third generation member of the U.S. Armed Forces, but most importantly, he met two life-changing individuals: Christ, and Cadet Dawn Meredith Grover. He also gained an interest in hybrid composites and set sights for another goal: to return to the Academy as an instructor. Donald received a Bachelor of Science in Engineering Mechanics in 1995 and was commissioned an Air Force 2nd Lt. Upon graduation, Lt Rhymer worked for three years as an Air-to-Surface Weapons Engineer at the National Air Intelligence Center. Prior to his change of station, Lt Rhymer was interviewed and accepted as an instructor in the Department of Engineering Mechanics back at the Academy. He accepted, and was offered a tour as a full-time graduate student at a civilian school by the Air Force Institute of Technology. Following in the footsteps of Major Larry Butkus, Donald attended Georgia Tech and graduated with a Master's of Science in Mechanical Engineering in December of 1999. For the second time, now Captain Rhymer returns to CAMP USAFA, only with a little more freedom.